Development of Metal Organic Frameworks for Adsorption of Organic Pollutants

By

MUHAMMAD USMAN

School of Chemical and Materials Engineering (SCME)

National University of Sciences and Technology(NUST)

2017

Development of Metal Organic Frameworks for Adsorption of Organic Pollutants

Name: Muhammad Usman

Reg. No: NUST201463887MSCME67814F

This thesis is submitted as a partial fulfillment of the requirements for the degree of

MS in Chemical Engineering

Supervisor Name: Dr. Tayyaba Noor

School of Chemical and Materials Engineering (SCME)
National University of Sciences and Technology (NUST)
H-12 Islamabad, Pakistan
February, 2017

Dedication

Dedicated to my Beloved Parents, Respected Teachers and Friends

Acknowledgments

Abstract

Today supply of clean water is one of the utmost significant universal issues due to ongoing economic expansion and the continuous upsurge in the worldwide population. Clean water sources are reducing each day because of contagion with various organic and inorganic pollutants. Fertilizers, organic dyes, phenols, plasticizers, detergents, pharmaceuticals, pesticides, and aromatics are typical toxins that should be removed from drinking and wastewater. Among different wastewater treatment approaches adsorption gives a simple, ease of equipment design, low cost and one of the most commonly used solution. Metal Organic Frameworks (MOFs) have appeared as a new class of adsorbent materials, which gained attention over the last two decades due to their large surface area, tunable pore size and ease of synthesis. They are reported to be potential candidate for the adsorption of dyes and heavy metals in waste water treatment. In present work, six metal organic frameworks have been synthesized by solvothermal process using nickel, cobalt and magnesium metals as inorganic part whereas oxalic acid and phthalic acid were used as organic linkers. Characterization of these lab prepared MOFs was done by FT-IR spectroscopy, XRD, SEM, and TGA analysis. Subsequently, these MOFs were studied for their adsorption capacity for three organic dyes namely, Methylene Blue (MB), Methyl Orange (MO) and Methyl Red (MR) from aqueous solution. The adsorption mechanism was studied in batch process by using UV-Visible Spectroscopy. Among series, Ni-Oxalic MOF showed highest capacity for adsorption of dyes from aqueous solution. Kinetic study of dyes adsorption by MOFs illustrates that adsorption process follow pseudo second order kinetic model.

Keywords: Metal Organic Framework, Solvothermal Method, Oxalic Acid, Phthalic Acid, Organic Dyes, Adsorption, Kinetics.

Table of Contents

List of Figures

List of Tables

Acronyms List

MOF	Metal Organic Framework
Ni-Oxalic	Nickel Oxalic Acid
Ni-PA	Nickel Phthalic Acid
Co-Oxalic	Cobalt Oxalic Acid
Co-PA	Cobalt Phthalic Acid
Mg-Oxalic	Magnesium Oxalic Acid
Mg-PA	Magnesium Phthalic Acid
XRD	X-ray diffraction
FTIR	Fourier Transform Infrared
SEM	Scanning Electron Microscopy
BET	Brunauer, Emmett and Teller
Methyl Orange	MO
Methylene Blue	MB
Methyl Red	MR
PSM	Post synthetic modifications
IRMOF	Isoreticular Metal Organic Frameworks
CPO	Coordination polymer of Oslo
PCN	Porous Coordination Network
SBU	Secondary building unit
BTC	1,3,5-BenzenetricarbOxalicylic acid
BTB	1,3,5-tris(4-carbOxalicyphenyl) benzene
BDC	1,4-BenzenedicarbOxalicylic acid
CUS	Coordinative unsaturated metal site
STP	Standard temperature and pressure
DMF	Dimethylformamide
DEF	Diethyl formamide

Chapter 1: Introduction

1.1. Background

In the 20th century, there has been significant rise in the study of porous hybrid organic–inorganic materials known as organic coordination networks. These materials can be prepared via self-assembly of a metal (a connector) and a ligand (a link) where connectors and links are combined through a metal–ligand bond to make porous crystalline structures. Surface structure of organic ligands is adjusted to higher porosity and increased surface area prone to provide good adsorbents [1].

One prominent characteristic of coordination networks is the opportunity to design the pores. Now there is a possibility to design the pores with specific size, just by selecting suitable ligands. Due to this feature, reactions that cannot be carried out in the solution phase can be done within the pores of hybrid coordination networks. A broad range of processes can be carried out in the pores of these materials [2].

Another aspect of these materials is their flexibility, which makes a distinction from the tough frameworks of zeolites and enables structural variation (guest exchange or chemical reactions within the pores) with no loss of its structural integrity. Therefore, X-ray crystallography and other spectroscopic methods can be utilized to monitor chemical reactions that occur in the pores [3]. In the beginning, porous and open-framework coordination networks had significant attention as post-zeolite materials. Recent growth of coordination networks is amazing in that many fascinating functions and properties are useful in a broad array of applications as well. For example, guest exchange, gas adsorption, structure alteration, selective separation, selective molecular detection, pore post-modification, catalysis, and gas storage have been reported [4]. Struggle of many researchers paved the way for finding a new direction to make materials having bigger cavities. For instance, if organic linkers could be placed instead of –CN group, a range of coordination networks having finely tuned cavities could be prepared. More than twenty years have occurred when the term "Metal-Organic Framework" first emerged in literature when Li and coworkers reported the structure of the MOF-5 in his paper [5].

1.2.   Introduction of MOF

Metal organic frameworks (MOFs) are only one of its kind castes of crystalline porous solids that have been considered extensively for several purposes, for instance, gas storage, heterogeneous catalysis, gas separation, adsorption and many more [6].

Usually, metal-organic frameworks are synthesized by compiling metal atoms or small metal-containing knots with multi dentate organic ligands by coordination bonds. Most MOFs have 3D structures include identical pores and an arrangement of conduits, which can be packed with guest materials such as solvents that are ensnared during production of MOFs. With appropriate removal of the trapped guest solvents, the porosity can be created [7–9].
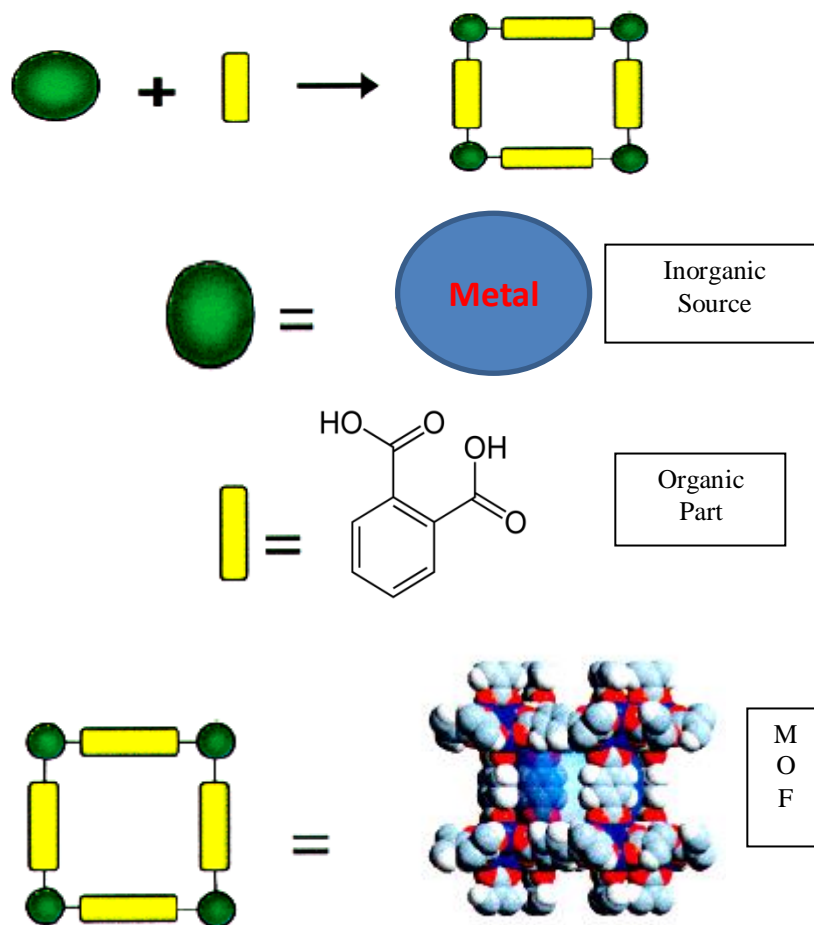
Figure 1.1 Schematic representation of different components of Metal Organic Framework

1.3. Classifications of Porous Solids

As of their helpful usages, Porous solids have scientific interest. Macro-Porous Mesoporous and Microporous are types of these porous solid materials. This classification is based on the pore size of these materials. Microporous solid have pore size of ≤ 2 nm. The range of mesoporous solids is 2 nm to 50 nm and for > 50 nm is recognized as macro porous. A leading example of the microporous materials is Zeolites which are crystalline Alumina silicates solid material [10].

Production of the desired, chemical, physical and architectural properties of MOFs depend upon chemical configuration of the ligand and the properties of the connecting metals. MOF materials are crystal networks having one, two, and three dimensional structures. The 2D and 3D configurations of Metal Organic Frameworks can show evidence of small voids or open channels [11].
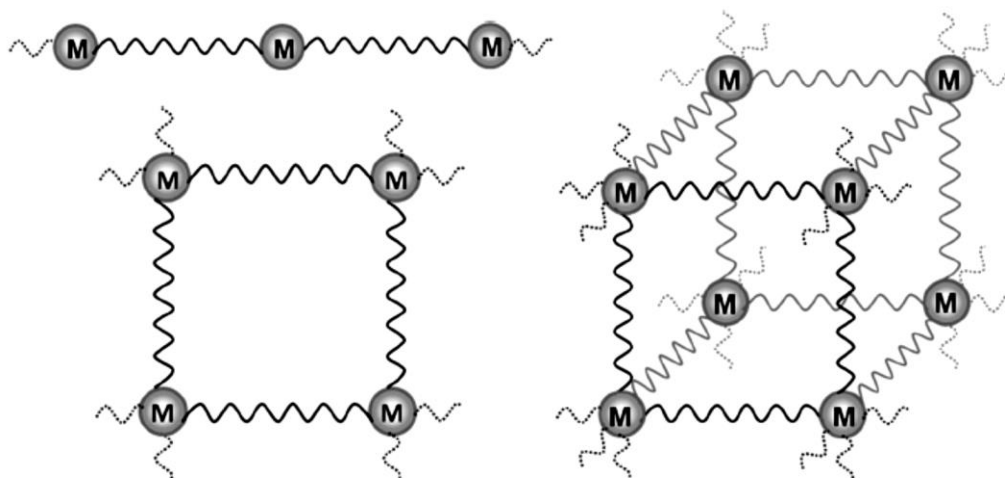
Figure 1.2 Representation of 1D, 2D and 3D MOFs [12]

1.4. Effects of Synthesis Routes on MOF Structure

MOFs can be prepared by using many methods including room temperature, solvothermal, hydrothermal, vapor diffusion, direct mixing, microwave heating, etc. The solvothermal scheme of MOF synthesis is commonly used; in a solvent system mixture of metal salt and organic ligands is heated. Ethanol, water, dimethylformamide (DMF) and di-ethyl formamide (DEF) are common solvents used in the synthesis of MOFs. Due to the tendency of dissolving reactants as well as deprotonating of carboxylic acids,

amongst these solvents formamides are popular. Along these parameters variables in the reaction conditions for example, reactants concentration, time, temperature and partial volume filling of the vessel are important considerations in MOF synthesis as well [12]. Temperature control and long reaction time are two main disadvantages of the solvothermal method [13].

1.4.1. Network Geometry

Network geometry of the MOFs are highly depending upon metal synchronization and the properties of the organic linkers. Distinctively, new MOFs can be prepared by changing the bridge or its functionalization, without altering the original topology. Transition metal ions offer coordination spots for the organic ligands [14].

Linkers are usually multidentate bridging ligands, containing a large selection of linking sites, with binding strength and direction of organic ligands exceptional to its topology. Inflexible ligands will be in control of the physical topologies during the synthesis process. Organic ligands require careful valuable studying because the structural properties of these porous materials are highly dependent upon them. For the synthesis of a definite network, selection of ligand, length of the ligand, number of binding sites and its flexibility must be considered [15]. Multidentate organic ligands containing N and O are widely used to construct these structures [16]. Various common paragons of N and O contributor ligands are shown in Figure 1.4. In relation to N & O ligands, the challenge was to manufacture the MOF with various rigid ligands. Character is determined by the product Ligand concentration, solvent polarity, type of anion, solubility, and temperature. [17].
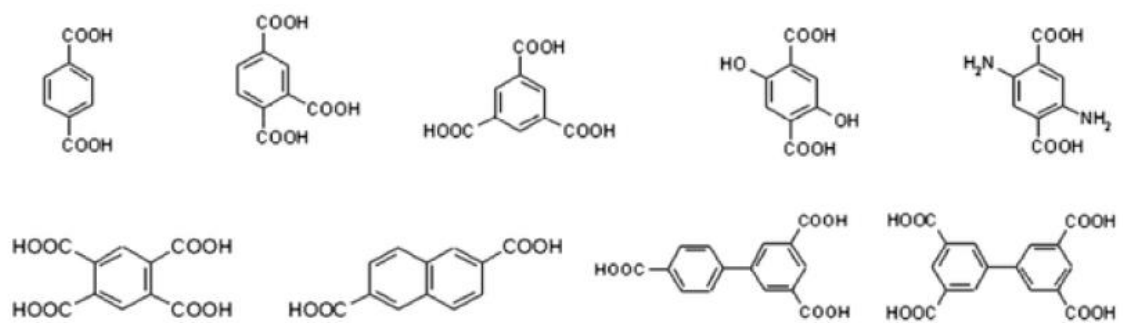
Figure 1.3 Common organic ligands used in MOFs synthesis

1.4.2. Effect of Secondary Building Units (SBU)

The preparation of MOF materials should not just selection of some raw materials and their synthesis but must have some insight look as how the final product is shaped by the combining of these raw reactants. A promising method in the normal fabrication of networks is using secondary building units (SBUs). The idea of SBUs as per structural units of MOFs was implemented from structure of zeolite. Secondary building units are complex molecular bunch units that are connected via organic ligands to form unmitigated porous systems. Preparation of many inorganic and organic SBUs with variable geometries is possible, due to this approach [18]. Some examples of SBUs from carboxylate Metal Organic Frameworks are represented in figure 1.6. Blue color indicates metal-oxygen polyhedral in inorganic units and red represents the polygon defined by carboxylate carbon atom. In the organic SBUs the polyhedrons to which organic ligands are combined, exposed in green.
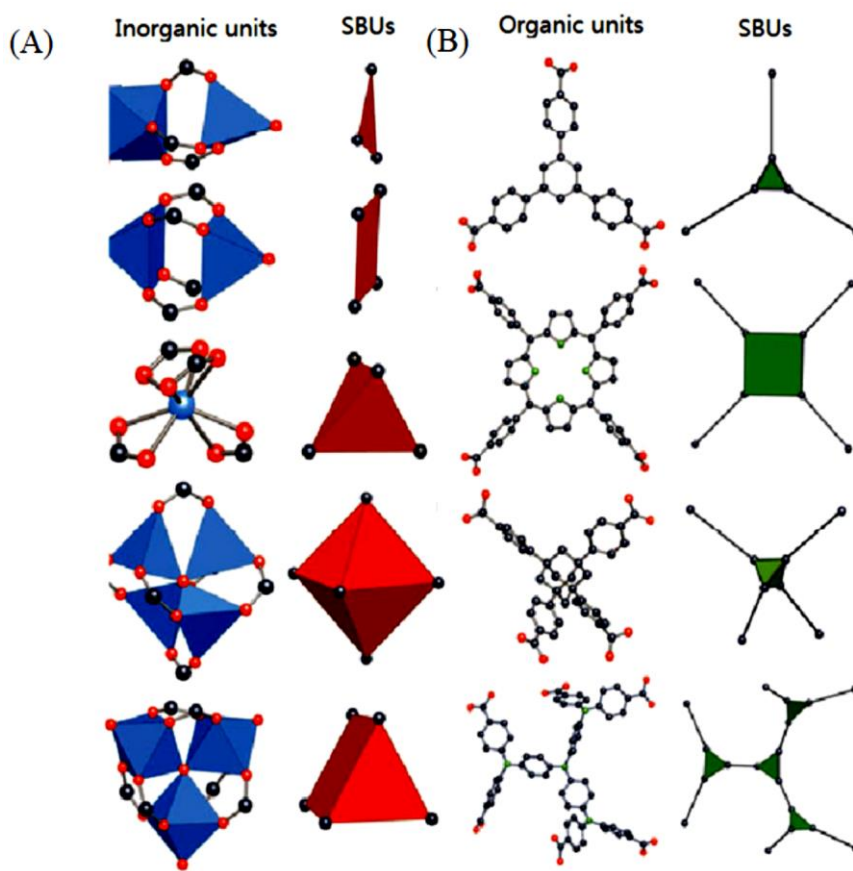
Figure 1.4 Examples of organic & inorganic units and their corresponding secondary building units (a) inorganic units (b) organic units [19]

1.5. Aim of Present Work

To understand the role of organic linkers and metal Oxides on structure formation of different MOFs is the main objective of the work presented in this MS thesis. Solvothermal technique required high temperature and temperature control mechanism; we tried to synthesize MOFs near ambient temperature and without any complex temperature control system.

Understanding the structural properties and comparison among these synthesized materials is also included in the main goal of the project.

Adsorption study of organic dyes Methyl Orange, Methylene Blue and Methyl Red on synthesized MOFs as well as Comparison in characteristics and percentage dyes removal of these MOFs are included in aim of this project.

1.5.1. Outline of the Thesis

1st Chapter includes the overview of Metal Organic Frameworks. Moreover, different types of MOFs and their features are also highlighted in this chapter. The challenges involved in the designing and synthesis of MOFs are discussed. Outline and Aim of the thesis is concluded at the end of 1st chapter.

2nd Chapter comprises of summery of the research work already carried out on MOFs for organic pollutant adsorption applications. Synthesis techniques of MOFs have also been discussed. Moreover, Different Applications and properties of MOF materials are also highlighted in this chapter.

3rd Chapter includes materials and methodology adopted for synthesis of MOFs. Characterization techniques adopted for determining MOFs properties are also discussed in this chapter.

In **4th chapter** the Results obtained from characterization techniques are discussed. Second part of this chapter includes the dyes adsorption study of MOFs. Comparisons between six synthesized MOFs in this work are also highlighted.

5th Chapter contains a precise summary of the entire MS research work and future recommendations are also discoursed.

Chapter 2: Literature Review

2.1. Removal of Organic Pollutants from Water

One of the most significant universal issue due to ongoing economic expansion and the continuous upsurge in world's population is the supply of clean water. Rapid growth of industrial plants causes worse environmental and pollution problems for mankind [19]. Waste from chemical plants, combustion byproducts, textile industries and dye manufacturing firms contain numerous type of pollutants. Ground, drinking, sewage and effluent water has experienced several non-biodegradable pollutants. Waste water treatment is an imperative field of study. Conventional waste water purification approaches containing chemical, physical and biological methods are unable to effectively remove these soluble pollutants due to their non-degradability and byproduct generation [20].

Wastewater created in many industrial processes holds toxic organic pollutants containing fertilizers, organic dyes, phenols, plasticizer, detergents, pharmaceuticals, greases, hydrocarbons, oils, pesticides and carbohydrates. All these pollutants have lots of varieties. For example, around 100,000 commercially existing organic dyes are chemically stable and generated 7×10^5 ton annually [21].

Dyes are pollutant chemicals that give colors to the material upon binding. There are various environmental problems such as increasing biochemical Oxygen, harmfully effecting aquatic life and blockage in sewage treatment plants, caused by the release of these organic dyes in the aquatic environment. Therefore, there is an immense need to reduce these organic dyes effectively and economically, prior to discharge wastewater into the environment. Intensive study is being done for selecting an appropriate method to overcome this issue. Existing technologies for wastewater treatment include photocatalytic decomposition [22], photolysis [23], ozonolytic [24], membrane filtration [25], biological treatment [26] and adsorption [27]. Chemical methods as well as membrane technologies require high running cost and often produce secondary toxic organic pollutants [28–30].

Among these approaches adsorption is the method of choice, which requires less operating temperature and various coloring materials can be removed instantly. There is a variety of adsorbent being used for subtraction of organic dyes from effluent water. Grainy activated carbon, zeolite, active diatomaceous earth and resins have gained a lot of attention for this purpose. However higher process cost, difficulty in regeneration, limited structures and porous architectures available for sorption narrow the practice of these well-established adsorbents [31].

Thus, researchers are concentrating at the synthesis and development of alternative novel adsorbents having flexible architectural properties. Metal Organic Frameworks are crystalline hybrid organic-inorganic materials assembled by combination of metal ions or small metal. In 1995, Omar Yaghi named this porous materials as MOF [32].

2.2. Synthesis of MOFs

Commonly, MOFs are synthesized in liquid phase, in which both metal salts and organic linkers are either dissolved in a solvent or solvent is introduced into a mixture of organic-inorganic mixture in a reaction vial. In this liquid phase, MOFs synthesis technique, selection of solvent is highly depending upon various aspects like, solubility, stability, reactivity etc [33].

Along with this liquid phase synthesis, solid phase synthesis is also very reported by researchers because it is faster and easier [34]. A summary of different routes for MOF materials preparation is demonstrated in figure 2.1.

2.2.1. The slow evaporation method

Metal Organic Frameworks are conventionally synthesized by this method. This technique generally does not require any external supply of energy. Even though, its major drawback remains that it needs more time contrast with other famous established methods. At a preset temperature, a solution of the starting materials is concentrated by slow evaporation of the solvent. Occasionally this technique involves a mixture of solvents rather than a single solvent which can boost the solubility of the reagents and can make the process faster by more rapidly loss of low-boiling solvents [35].

8
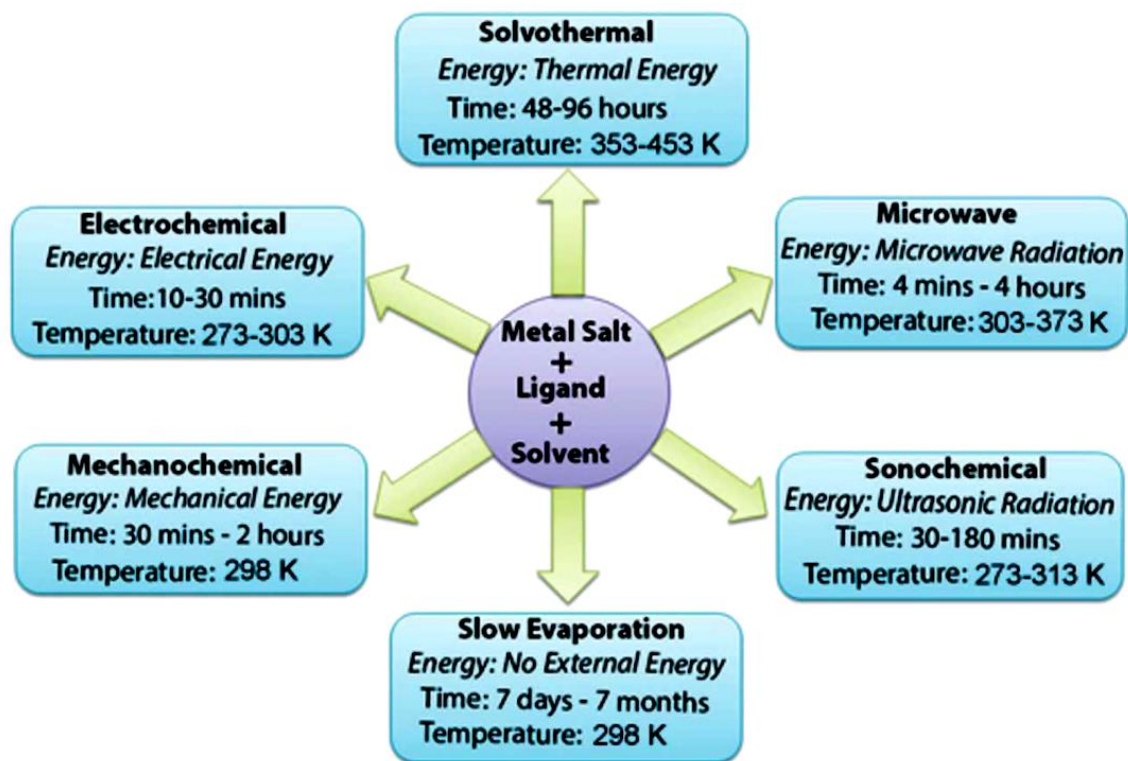
(a)
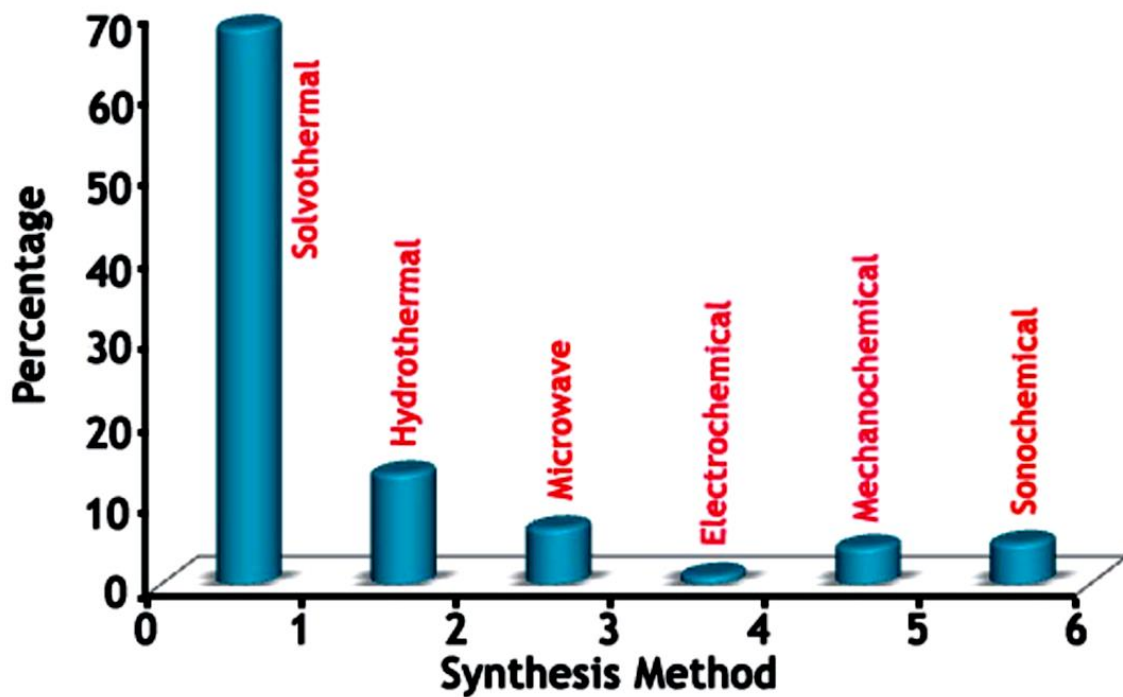
(b)

Figure 2. 1 (a) Synthesis routs for MOFs preparation (b) Percentage summary of different techniques [34]

2.2.2. The Solvothermal Method

In a closed reaction vial solvothermal reactions are carried out at pressure above the boiling point of the solvent. To a certain extent unexpected chemical changes are occurred in various starting materials under conditions of solvothermal route for MOFs synthesis, that are often due to the formation of Nano scale morphologies that are not realizable by usual methods. Mainly organic solvents with high boiling points have been used for solvothermal reactions. DMF, acetone, DEF, methanol, acetonitrile, ethanol, etc. are the most commonly used organic solvents. Commonly, lower temperature reactions are carried out in glass vials and reactions completed at temperatures higher than 600 ^{o}C need Teflon-lined autoclaves. [11,12,36].

2.2.3. The Microwave-Assisted Method

A very rapid synthesis of MOF materials can be achieved by using Microwave-assisted synthesis technique. The procedures involved in this method have been used comprehensively to fabricate Nano size metal Oxides. Heating a solution mixture by microwave for 1-2 hours to create crystals of Nano size is concerned in the procedure of Microwave-assisted method. This method is also known as "microwave-assisted solvothermal synthesis" for MOFs preparation. Similar crystals structures can be achieved by this process as that of formed by the regular solvothermal procedures, but the preparation is much faster [37].

2.2.4. The Electrochemical Method

Improvement and understanding of new rapid synthetic procedures for MOFs synthesis is ongoing day by day especially for the sake of rapid creation of large MOF crystal in large amount, although by change solvent and pH at room temperature there is a opportunity to synthesis large MOF crystal materials. Electrochemical synthetic process is one among them; it does not need any metal salt and proposes nonstop production of the product that is the most important benefit in an industrial process. Metal ion is provided by anodic termination into synthesis mixtures that consist of organic linkers and/or electrolytes, is the basic principle of electrochemical synthesis [38].

2.2.5. The Mechanochemical Method

Mechanochemical procedure involves no solvent for MOFs preparation. In this method, a chemical reaction is performed using mechanical force. In modern synthetic chemistry, formation of bonds by simple, environment friendly and economically is of great interest. This method involves, in a ball mill precise mixtures of organic linker and inorganic metal are ground together to produce the desired MOF. By using this technique, Pichon et al prepared first Cu-is nicotinic acid MOF, in 2006. To prepare MOF materials, microwave heating along with its fast reaction time and microcrystal products can also be used. [39]

2.3. Applications of Metal Organic Frameworks

Metal Organic Frameworks have numerous uses comprising in storage, separation, magnetic, catalysis, dye degradation and biomedical applications.

Starting materials should be sensibly selected before synthesizing of MOFs materials, for achieving the anticipated properties, the. The preparations of MOFs are fairly like the synthesis of organic polymers, where the physical characteristics of the polymer are highly depending upon nature of the monomer, which succeeds the properties of MOFs. Some applications such as dye adsorption, gas storage, gas separation, and magnetic properties will be discussed in this chapter.

2.3.1. Applications of MOFs in Dye Removal

Adsorption techniques are extensively used to remove certain organic pollutants from waters, especially those that are not easily biodegradable. Dyes represent one of the challenging groups [40]. Haque and coworker were the first to study the MOFs in the adsorption/removal of azo dyes in 2010 [41]. MOF-5 has been used to adsorb thiophene derivatives. Harmful cationic dye, anionic dye named as methylene blue and methyl orange respectively, were carried out on MOF-235. Adsorption of xylene orange from aqueous solution via MOF-101 has also been reported [42,43].

 MIL-100–Fe/Cr MOFs were also utilized to check the impact of metal ions framework in dyes adsorption of MO and MB by Tong et al [44].

2.3.2. Applications of MOFs in Hydrogen Storage

Water is the only product achieved from combustion of hydrogen with air, without any harmful product; this fact gives emphasis to the hydrogen economy [45]. Storage of Hydrogen in porous MOFs is due to several features of these porous materials, for example high surface area, less weight, functionalized polar groups, and open metal centers. [46].

Hydrogen storage capacity have been verified by more than 300 MOFs. One of them is MOF-177, which is built from $[Zn_4O]$ clusters, representing 7.5 wt. % gravimetric H_2 uptake at 70 bar and 77 K. MOF-5 is added famous zinc carboxylate based MOF, retains a BET surface area of 3800 m^2 g^{-1} and takes up 7.1 wt. % of H_2 at 40 bar and 77 K [47].

Mostly MOF materials with open metal sites which enable stronger collaborations between the nodes of metal ion and H_2 molecules. This is the primary reason behind the high Hydrogen storage in this encouraging group of materials. Additionally, theoretical calculations have suggested that MOFs doped with metal ions can improve the H_2 storage ability [18,48–50]

2.3.3. Applications of MOFs in Carbon Dioxide Storage

Previous, zeolites and activated porous carbons were intensively utilized for CO_2 adsorption, Metal Organic Frameworks, have now selected and considered as probable adsorbents Higher internal surface area with polar functional groups [51].

MOF-210 experienced highest surface area (10450 m^2 g^{-1}) and had CO_2 acceptance value of 2400 mg g^{-1} (74.2 wt%, 50 bar at 298 K) which beats any other porous material [52]. Occurrence of polar groups in the structure of MOFs like NH_2 or N comprising organic heterocyclic remains on the pores of material is useful for high CO_2 storage compared with un functionalized correspondents. BioMOF-11 showed 15.2 wt% CO_2 uptake and reveals the influences of an N heterocycle [53].

Free NH_2 as well as un-coordinated N result tetrazole molecule within the framework. Another example of this class is ZTF-1,ndisplays high CO_2 uptake/storage, 14.4 wt%, at 1 bar and 298 K [54].

2.3.4. Applications of MOFs in Gas Separation

Separation of gas can be done by means of selective adsorption because selective adsorption is based on different attractions at the specified situation. Kinetic, Molecular sieving, Thermodynamic equilibrium and Quantum sieving effects are the main mechanisms responsible for gas separation by using solid adsorbents [55].
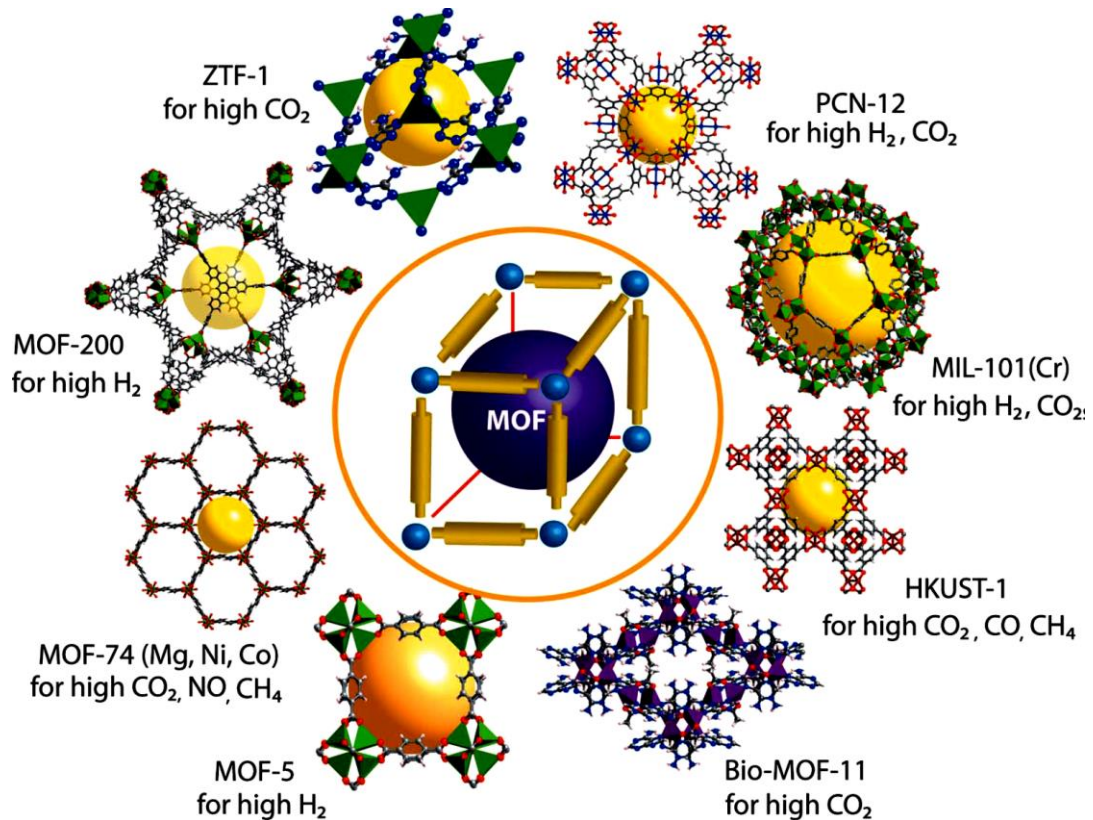
Figure 2. 2 Schematic illustration of important testified MOFs known for high gas storage capacity [55]

The post synthesized tunability of MOF materials make exceptional because in zeolites pores are difficult to modify due to its rigid tetrahedral Oxalic frameworks [56].

In flexible MOF Materials guest molecules appear as exterior incentives on the transformation in structural process. In the closed state the pores are typically not offered for guest particles but it expands and become available when certain type of guest particles is familiarized. This procedure is known as 'gate opening process'' and the pressure at that point when pores expand is named as 'gate opening pressure' [57].

MIL-53 MOF solid shows a breathing experience on hydration and dehydration processes. It has little uptake of CO_2 at 10 bar but it offered a distinct high uptake between the pressure of 12-18 bar range. Below 20 bars, there was no receipt of CH_4 and this was due to the non-polarity and the repulsive forces of water molecules in the framework. So MIL-53 and other MOFs of this category have tremendous gas separation applications [58].

Along with these applications and properties of MOFs, extensive literature is reported about this extensive research area. Conclusions / Findings of specifically removal of organic pollutants by using MOFs from some selected research papers are highlighted in table below:

Table 2. 1 Literature Survey of MOF Synthesis & Adsorption Applications

Authors	Year/Journal	Title	Findings
Gre´gorio Crini	2006 (Bioresource Technology)	Non-conventional low-cost adsorbents for dye removal: A review	Different Technologies and adsorbent available for color removal from waste water.
Gerard Ferey	2007 (Chemical Society Reviews)	Hybrid porous solids: past, present, future	Fundamental knowledge of hybrid porous solids, their advantages, their new routes of synthesis and the structural concepts.
G. Limousin J.P. Gaudet & M. Krimissa	2007 (Applied Geochemistry)	Sorption isotherms: A review on physical bases, modeling and measurement	Mechanisms involved in transfer of substances from a mobile phase (liquid or gaseous) to a solid phase.

Authors	Year/Journal	Title	Findings
Inayat Ali Khan, Amin Badsha	2014 (International Journal of Hydrogen Energy)	A copper based metal-organic framework as single source for the synthesis of electrode materials for high-performance super capacitors and glucose sensing applications	Room Temperature Synthesis Method, adopted procedure for this work
Alireza Abbasi, Mohammad Soleimani	2015 (Inorganica Chimica Acta)	New interpenetrated mixed (Co/Ni) metal-organic framework for dye removal under mild conditions	Synthesized MOF exhibited good activity and stability during the color removal process under mild conditions.
A. Majedi, F. Davar, A. R. Abbasi	2016 (International Journal of Nano Dimensions)	Metal-organic framework materials as nano photocatalyst	MOFs have an ability to replace the traditional photo-catalysts which have some drawbacks such as low quantum yield and UV source.
Ali Ayati, Mahdi Niknam Shahrak & Mika Sillanpaa	2016 (Chemosphere)	Emerging adsorptive removal of azo dye by metal organic frameworks	Adsorption kinetic and isotherm of azo dyes onto the MOFs mostly followed the pseudo-second order & Langmuir models.
Lei Shi, Liping Hu, & Jingli Xu	2016 (Journal of Dispersion Science and Technology)	Adsorptive Removal of Methylene Blue from Aqueous Solution using a Ni-Metal Organic Framework Material	85.08% removal of MB achieved by adopting UV Spectroscopy Batch adsorption procedure.

Chapter 3:   Experimental

3.1.   Materials Used

Nickle Nitrate Hexahydrate and Cobalt Nitrate Hexahydrate were purchased from commercial supplier (DAEJUNG) both having 97% purity. Above 99% pure N, N-Dimethylformamide was bought by local supplier (MERK). Triethylamine, Oxalic Acid, Phthalic Acid and Magnesium Nitrate Hexahydrate were purchased from three different local vendors MERK, Fischer Scientific and Sigma-Aldrich respectively, with min 99% purity. All these chemicals are used as received from these resources without any further refinement.

Table 3. 1 Physicochemical Properties of materials used in synthesis of MOFs

Sr. No	Chemicals	Molecular Weight $(\frac{g}{mol})$	Boiling Point (^0C)	Melting Point (^0C)
1	Oxalic Acid $C_2H_2O_4$	90.03488	145	103
2	Phthalic Acid $C_8H_6O_4$	166.13	210	207
3	Cobalt Nitrate Hexahydrate $Co(NO_3)_2 \cdot 6H_2O$	291.03	74	55
4	Nickle Nitrate Hexahydrate $Ni(NO_3)_2 \cdot 6H_2O$	290.79	136	57
5	Magnesium Nitrate Hexahydrate $Mg(NO_3)_2 \cdot 6H_2O$	256.41	330	89
6	Dimethylformamide (DMF) C_3H_7NO	73.09	153	-61
7	Triethylamine $(C_6H_{15}N)$	101.19	89.5	22

3.2. Synthesis Procedure of MOFs

The Ni-Oxalic, Co-Oxalic and Mg-Oxalic MOFs was synthesized by using room temperature synthetic technique in reaction vial as described by Amin Badshah et al [61]. In this typical procedure, Metal solution is made by dissolving 0.72g amount of each Nickle, Cobalt and Magnesium Nitrate Hexahydrates, separately in 20mL of DMF. Acid solution is made by dissolving 0.21g each of Oxalic Acid in 10 mL of DMF. Tri-Ethyl-Amine (TEA) was added to this Acid solution to yield a clear solution.

Hence, three acid solutions along-with three salt or metal solutions were prepared. Each acid solution was agitated at room temperature and its corresponding salt (metal plus solvent) solution was inserted drop wise into it. Finally, precipitates of MOF were gained by filtration, washed using DMF and dried at room temperature ($< 35^{o}$C).

The Ni-PA, Co-PA and Mg-PA MOFs was synthesized by using autoclave synthetic technique. In this procedure, Metal solution is made by dissolving 0.71g amount of each Nitrate Hexahydrate separately in 20mL of DMF. Acid solution is made by dissolving 0.21g each of Phthalic Acid in 10 mL of DMF. Similarly, like above procedure, Tri-Ethyl-Amine (TEA) was added to this Acid solution to make a clear solution, Hence, three acid solutions and three salt or metal solutions were prepared. Each acid solution was agitated and its corresponding salt (metal plus solvent) solution was inserted drop wise to it. Final solution was kept in autoclave for four hours at 120 ^{o}C to make precipitates. Finally, precipitates of MOF were gained by filtration, washed with DMF and dried.

Metallic Organic Frameworks (MOFs) synthesized by combining Nickel Nitrate Hexahydrate (Inorganic part) and Phthalic Acid (Organic part) is named as Ni-PA MOF. MOFs synthesized by combining Nickel Nitrate Hexahydrate and Oxalic Acid named as Ni-Oxalic MOF. Similarly, Table 3.2 contains the list for all the lab prepared MOFs along with their specifications.

Sr. No	MOF	Organic linker	Metal source	Solvent
1	Ni-Oxalic	$C_2H_2O_4$	$Ni(NO_3)_2 \cdot 6H_2O$	C_3H_7NO
2	Co-Oxalic	$C_2H_2O_4$	$Co(NO_3)_2 \cdot 6H_2O$	C_3H_7NO
3	Mg-Oxalic	$C_2H_2O_4$	$Mg(NO_3)_2 \cdot 6H_2O$	C_3H_7NO
4	Ni-PA	$C_8H_6O_4$	$Ni(NO_3)_2 \cdot 6H_2O$	C_3H_7NO
5	Co-PA	$C_8H_6O_4$	$Co(NO_3)_2 \cdot 6H_2O$	C_3H_7NO
6	Mg-PA	$C_8H_6O_4$	$Mg(NO_3)_2 \cdot 6H_2O$	C_3H_7NO

a

20 ml DMF

0.72g of Ni/Co/Mg metal precursor

TEA — 10 ml DMF

0.21g of Oxalic Acid

[Metal Solution]

[Acid Solution]

Adding metal solution drop wise in acid solution

Mix Solution
Stirring, 4 hrs. → Filtration

MOF ⇐ Washing with DMF & Drying

b

TEA

0.71 g Inorganic Metal — 20 ml DMF 0.21 g Organic Linker — 10 ml DMF

[Metal Solution]

[Acid Solution]

Adding metal solution drop wise in acid solution

Mix Solution
Stirring, 4 hrs. → Autoclave (120°C, 4 hrs. → Filtration

MOF ⇐ Drying & Washing ⇐

19

Figure 3. 1 Schematic representation of MOFs synthesis (a) Oxalic Acid MOFs (b) Phthalic Acid MOFs

3.3. Characterization Techniques

Characterizations of synthesized MOFs has been done by various characterization techniques such as SEM, XRD, TGA, FTIR and UV Spectroscopy.

The details of these characterization techniques are described below:

3.3.1. Scanning Electron Microscopy (SEM)

SEM is the most commonly used electron microscope. A ray of high energy electrons is focused on the materials surface and examines the microscopic structure of the materials. The electron ray generates different signals at the surface of the material, which delivers the information about the morphology (texture) and chemical composition of the sample. Mostly information is gained over the chosen/selective area of the sample surface. Analysis of selected points on the sample surface can also be performed by SEM. The function of SEM is very like the electron probe microscope.

When a high-energy beam of electron is focused on the solid surface, kinetic energy of the electrons is dispersed. Sample image is mainly formed by secondary electrons and backscattered electrons. Backscattered electrons are more valuable in phase discrimination and secondary electrons are more important for viewing the morphology and topography of the sample.

The most common SEM mode is detection of secondary electrons discharged by atoms excited by the beam of electrons. The number of secondary electrons that can be detected greatly depends on specimen topography. By scanning the sample and collecting the secondary electrons that are emitted using a special detector, an image displaying the topography of the surface is created. X-rays are formed by the collision of incident electrons and the electrons present in shells of the sample atoms [62]. The working principle of SEM is showed in figure 3.2. SEM analysis provides the following information about the sample:

Morphology: related to the size and appearance

Topography: related to the surface characteristics of the sample
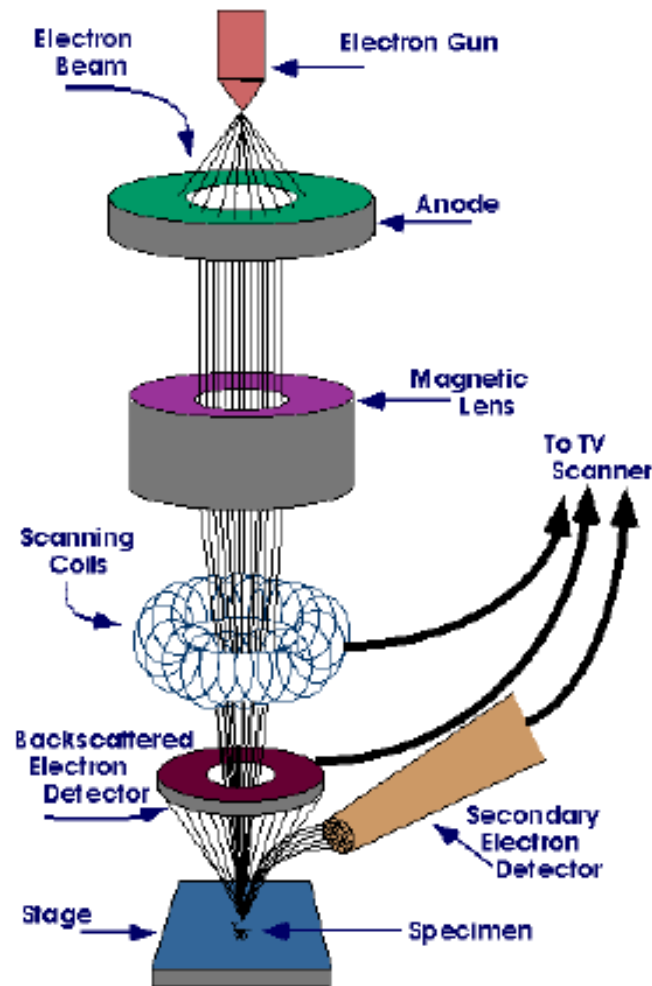
Figure 3. 2 Working principle of SEM [63]

3.3.2. X-Ray Diffraction (XRD)

XRD is a method used to illustrate the crystalline structures of solid samples. The size of crystallites, lattice parameters and other important information related to crystals can be obtained by interpreting the results. X-rays are the electromagnetic radiations having a wavelength of ~1 Å, shorter than ultraviolet but longer than γ-rays.

Working principle of this technique shows that X-rays are formed when a high-energy charged electron beam on a solid surface / target, normally copper or molybdenum.

Upon interaction of electron, the inner shell electrons in atoms can be evicted by ionization process. Outer orbital will instantly fill the empty site by a free electron and an x-ray photon is discharged owing to the energy released in the conversion. The relationship between the energy of radiation and wavelength is publicized in the following equation:

$$E = \frac{hc}{\lambda}$$

h represents Planck's constant while c is for speed of light in vacuum.
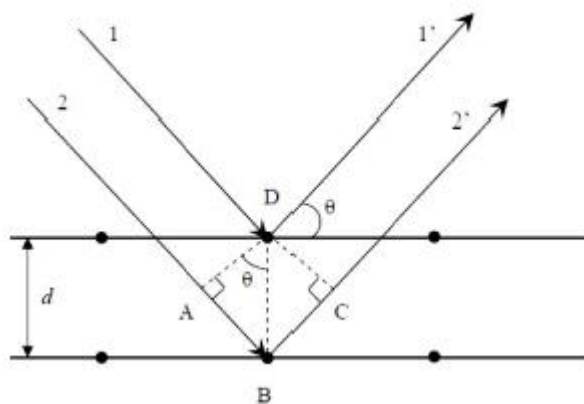
Figure 3. 3 description of Bragg's Law

Bragg's law is a simple formula to understand the process of diffraction and is widely used in crystal diffraction as well. Using Debye-Scherrer equation we can calculate the crystallite size of the crystals. Each crystalline material has its own unique X-ray pattern which is used as a finger print for its identification.

3.3.3. Fourier Transform Infrared (FTIR) Spectroscopy

The term Fourier transform is used for this type of spectroscopy because mathematical process that is Fourier transform is required to obtain actual spectrum from raw data. FTIR is used to perform quantitative and qualitative analysis of organic and inorganic samples. It is an efficient method to detect the functional groups and to identify the type of chemical bonds present in the sample under test.

In FTIR analysis infrared radiations interact with the sample. Some radiations are absorbed by the sample and some are transmitted through the sample. Based on absorbed and transmitted radiations, spectrum is obtained known as FTIR spectrum. The resulting spectrum creates a finger print of the sample, used to identify the sample. The frequency range is measured in terms of wave number and varies from $4000 - 400$ cm^{-1} [64].
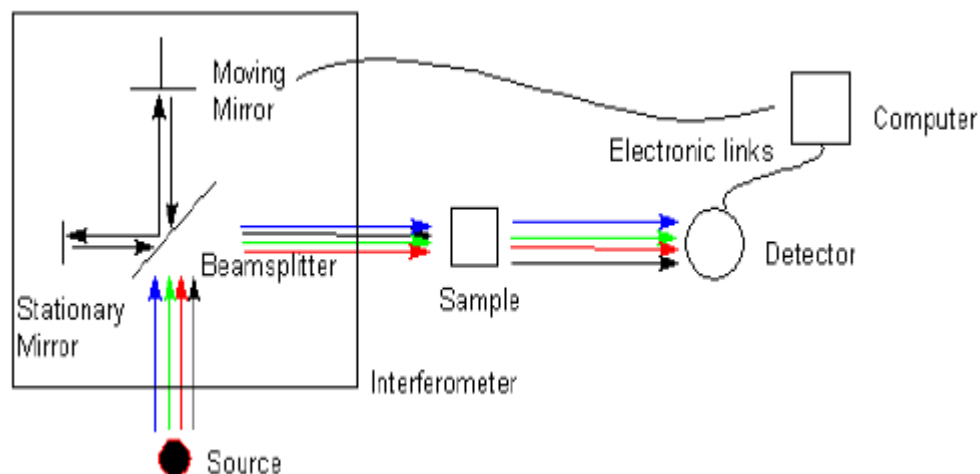
Figure 3. 4 Working Principle of FTIR [65]

The covalent bonds in a flexible, unlike rigid bonds, are flexible and always in a state of a vibration. Vibration could be bending or stretching. The vibrational motion possessed by these molecules is the characteristics of their respective atoms. All organic compounds are capable of absorbing IR which matches to their vibration. IR spectrum obtained is a graph between percentage transmittance and wavenumber presenting the variation of percentage transmittance with the frequency of the infrared radiation.

3.3.4. Thermogravimetric Analysis (TGA)

Thermogravimetric analysis abbreviated as TGA is a thermal analysis technique in which weight loss or weight gain of the sample powder is observed with time or increasing temperature. Investigation is done in presence of Nitrogen or Oxygen environment. The changes in chemical like dehydration, solid-gas reactions, chemisorption, decomposition etc. and physical properties like desorption, absorption, adsorption, vaporization, sublimation etc. are determined.

When materials are subjected to heat, physical and chemical changes occur. The weight of the material is either increased or decreased. Thermogravimetric analyzer consists of a pan placed in a programmable furnace.
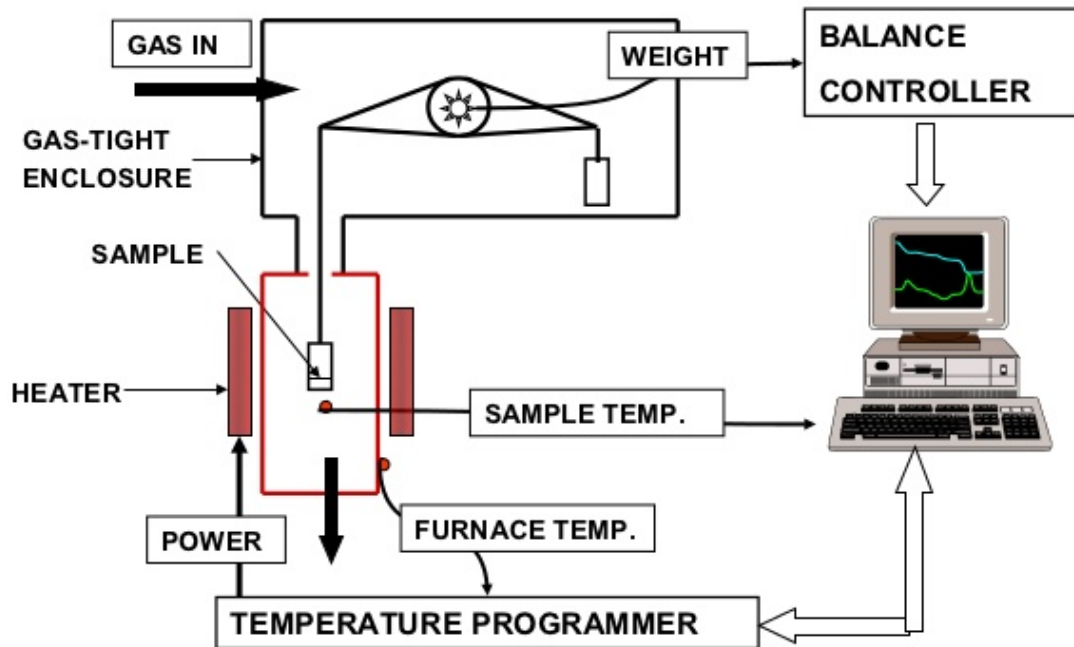
Figure 3. 5 Schematic Diagram of TGA [66]

This pan is supported by a sensitive precision balance. The specimen is placed onto the pan and a heating rate and a temperature range up to which changes is the material is to be observed is given to the furnace. The furnace is heated from a lower limit of the temperature range (usually from room temperature), reaches the maximum point and then it is cooled. The mass change is monitored during the heating and cooling process. The environment of the furnace is controlled by an inert or a reactive gas.

The data obtained from TG analysis of the sample enables the interpretation of loss of volatile components in the sample, its thermal stability, and decomposition. The data obtained is plotted in the form of a graph between increasing temperature (x-axis) and percentage in weight loss (y-axis). In the given temperature range, if a graph shows a straight line meaning no weight change, this means that the species is thermally stable. Sometimes an initial weight loss is shown in the graph and then the line becomes

straight which means the species is thermally unstable at low temperature and then becomes stable. The data from TG analysis also provides information about the maximum use temperature of the material beyond which the material will degrade. It also provides information about reaction kinetics, degradation mechanism, the presence of inorganic content in material and decomposition patterns [65].

3.3.5. Ultraviolet–Visible spectroscopy

UV-Vis spectroscopy is an analysis technique in which uses visible (400 nm- 00nm) and ultraviolet (190 nm-40 nm) regions of the electromagnetic spectrum to obtain information about organic molecules. It is performed to determine impurities in an 80 sample. Additional peaks other than the specimen substance's peak indicate the presence of impurities. It gives information about structural elucidation of the specimen. Combination and location of peaks help us to analyze whether saturation, unsaturation, and hetero atoms exist in the specimen or not. Quantitative analysis of compounds can be performed which absorb UV or Visible radiation using Beer-lambert law.

The spectrum obtained by UV-VIS spectrophotometer is compared to spectra of known compounds. Qualitative analysis of functional group can also be determined as the presence of a band at certain wavelength determines the presence of a group.
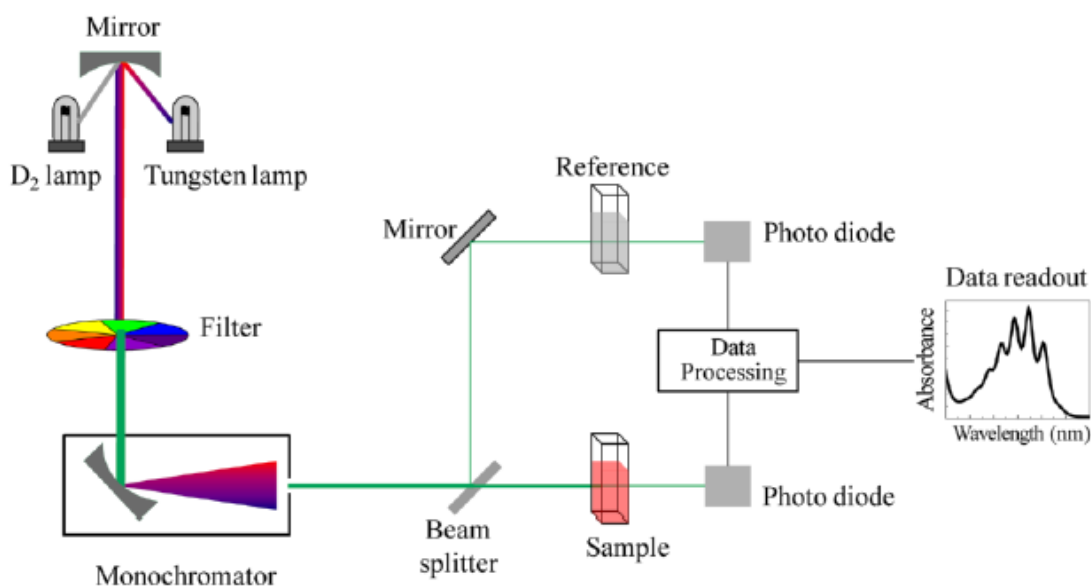
Figure 3. 6 The working principle of UV-Vis Spectrometer [67]

When molecules that possess non-bonding or π electrons are irradiated to UV-Vis light, the electrons get excited to higher anti-bonding orbitals. Lesser the energy gap between HOMO and LUMO of a material, easier is the excitation of electrons by longer wavelength radiations.

When a molecule with an energy gap between HOMO-LUMO equal to Δ is exposed to radiation with a wavelength corresponding to Δ, the electron is jumped from HOMO to LUMO. This is referred to as σ - σ* transition. The plot between the wavelength of x-axis and absorbance on the y-axis is obtained and analyzed [66]. The spectrum obtained by spectrophotometer is always compared to spectra of known compounds that are already studied.

(a) (b)
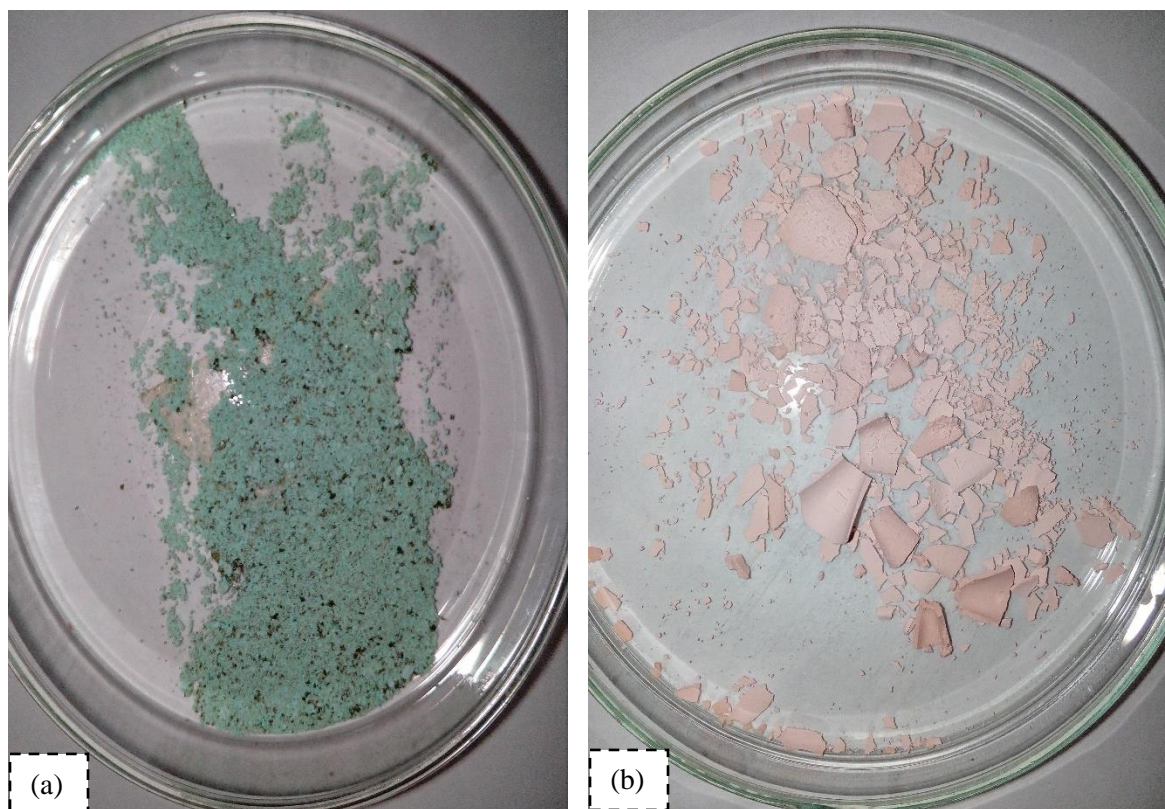
Figure 3. 7 Image of as synthesized (a) Ni-Oxalic MOF (b) Co-Oxalic MOF

Chapter 4: Results and Discussion

The crystal structures of lab synthesized MOFs were confirmed by using powder X-Ray Diffractometer (STOE - Germany), model θ - θ (theta -theta), at 0.02 step size and scan speed of 0.5 sec per step with CuKα radiation of wavelength (λ=1.54060Å) operated at 40 kV and 40 mA over the 2θ range of 10-70°.

The shapes and morphologies of these materials were verified by Analytical Scanning Electron Microscope (JEOL – Japan), model JSM-6490A. As MOF samples are nonconductors so prior to SEM analysis, 250Å gold coating were done by Auto Quick Coater (Ion Sputtering Device) model JFC-1500 made by JEOL – Japan.

Loss in mass of a MOF substances are observed as a function of temperature or time in thermogravimetric analysis. Pyris Series Diamond (German) TGA/DTA equipment was used for this analysis with Nitrogen gas at 20.0 ml/min. Three to five mg of each MOF sample was utilized in TGA analysis. Action occurs Immediately while N_2 gas switched to set flowrate with heat from 25.00°C to 700.00°C at 10.00°C/min temperature rate.

Fourier Transform Infrared Spectroscopy (FTIR) is used to perform quantitative and qualitative analysis of organic and inorganic samples. It is an efficient method to detect the functional groups and to identify the type of chemical bonds present in the sample under test. Perkin Spectrum 100 FT-IR Spectroscopy was used in this work via KBr pellet method.

Batch adsorption experiments was performed by using UV-VIS Spectrophotometer (PG Instruments UK), model T-60U.

In this chapter, results obtained by using above mentioned characterization techniques are discussed in detail.

4.1. Scanning Electron Microscopy Analysis

SEM is a technique that used to study the microstructure of nanoparticles of a matter. Each of the lab prepared Metallic organic framework (MOF) was analyzed by Scanning Electron Microscopy (SEM) to investigate the surface morphological features and evaluation of average particle size.

The Analytical Scanning Electron Microscope (JEOL – Japan) of model JSM-6490A was utilized for confirming morphological structure. As MOF samples are nonconductors so prior to SEM analysis, 250Å gold coating were done by Auto Quick Coater (Ion Sputtering Device) model JFC-1500 made by JEOL – Japan.

Figure 4.1 displays the simple organic framework of Oxalic acid with Nickel indicating attractively arranged particles with well-defined pores. Moreover, it has highly porous geometrical shape with average particle size for Ni-Oxalic MOF was found 68.68 nm which is in contrast with other reported work [67].

Figure 4. 1 SEM images of Ni-Oxalic MOF (a) Lower magnification (b) Higher magnification

More spherical shaped a vital crystal size diminution as Ni includes in the structure were noticed with the secondary electron detector. The smaller crystal size examined for Ni-Oxalic MOF could support the XRD signals broadening, detected before.

Average pore diameter for Ni MOF revealed by SEM analysis was 39.59 nm. Therefore, this material lies in mesoporous range. (<50nm)
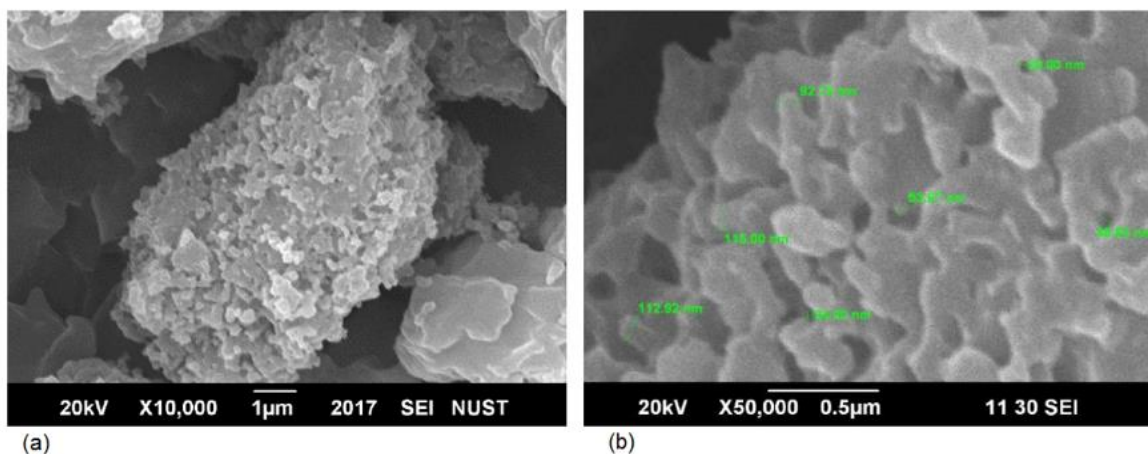
Figure 4. 2 SEM images of Co-Oxalic MOF (a) Lower magnification (b) Higher magnification
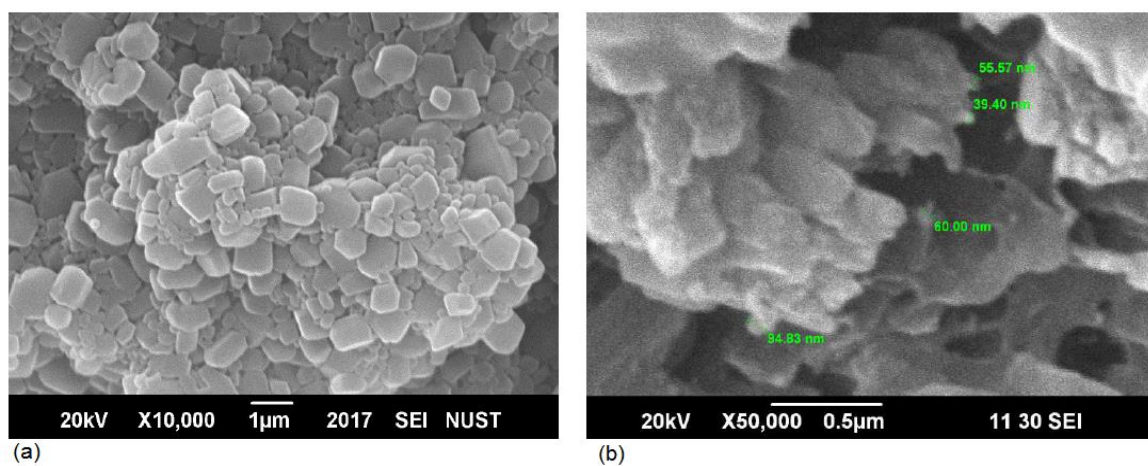
Figure 4. 3 SEM images of Mg-Oxalic MOF (a) Lower magnification (b) Higher magnification

Needle like shaped crystal structure was observed for Co-Oxalic MOF with 77.9 nm average particle diameter. High magnification SEM image shows irregular flake like shape for Co MOF.

The cubical shape of Mg-Oxalic MOF crystals was clearly seen in the figure 5. The average crystal size of Mg-Oxalic MOF was 62.44 nm with showing some aggregation.

The morphology of as-synthesized Co and Mg based MOF materials was in harmony with other SEM images published for these type of materials [68].
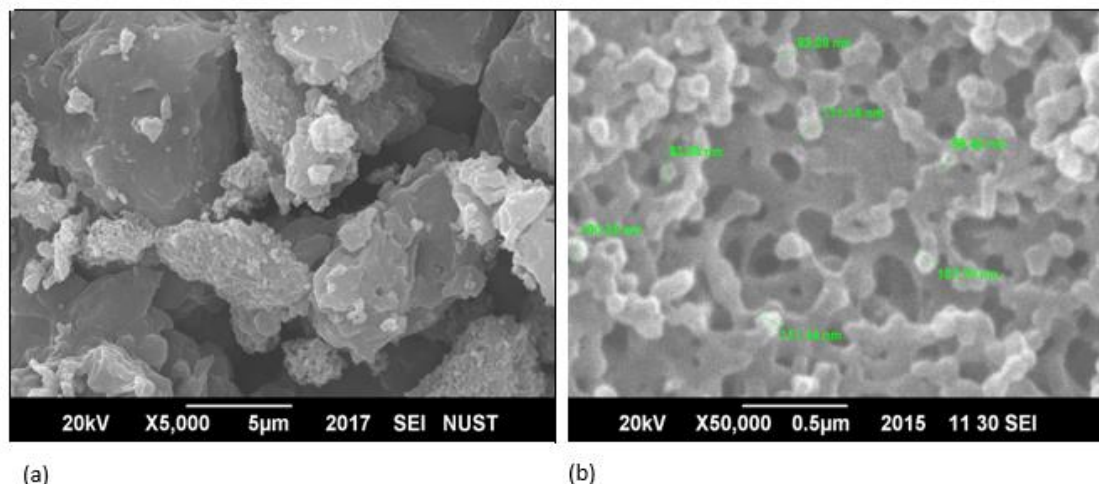
Figure 4. 4 SEM images of Ni-PA MOF (a) Lower magnification (b) Higher magnification
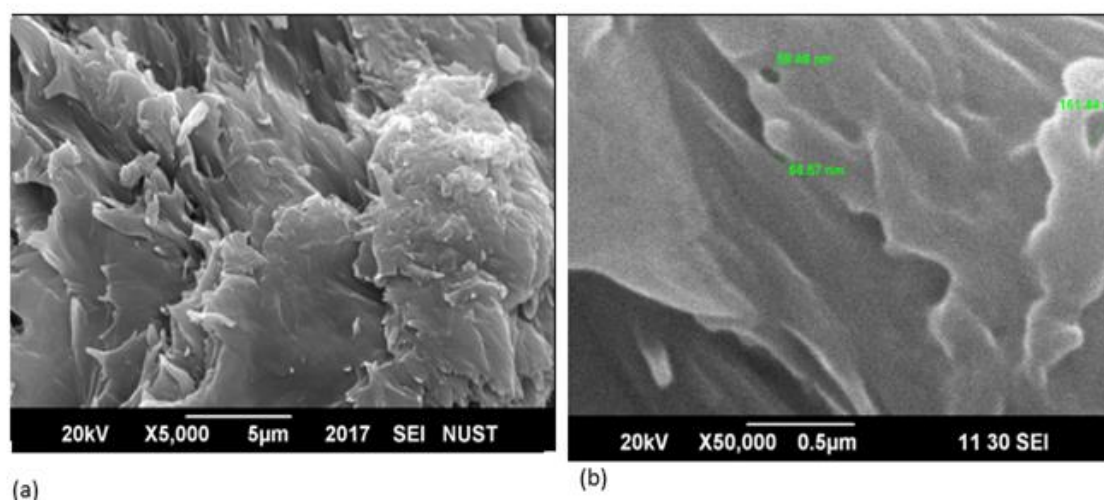
Figure 4. 5 SEM images of Co-PA MOF (a) Lower magnification (b) Higher magnification

The simple organic framework of Phthalic acid with Nickle displays attractively arranged particles with well-defined pores and highly porous geometrical shape. Average particle size for Ni-PA MOF was found 68.68 nm which is in contrast with other reported work [48,69]. More spherical shaped vital crystal size diminution as Ni includes in the structure were noticed with the. Average pore diameter for Ni MOF revealed by SEM analysis was 55 nm. Needle like shaped crystal structure was

observed for Co-PA MOF with 77.9 nm average particle diameter. High magnification SEM image shows irregular flake like shape for Co MOF. The cubical shape of Mg-PA MOF crystals was clearly seen in the figure 5. The average crystal size of Mg-PA MOF was 62.44 nm with showing some aggregation. The morphology of as-synthesized Co and Mg based MOF materials was in harmony with other SEM images published for these type of materials [70].

Figure 4. 6 SEM images of Mg-PA MOF (a) Lower magnification (b) Higher magnification

Among these MOFs materials, clear pore size distribution can be identifying only for the case of Ni-Oxalic MOF. MOF synthesized by using Cobalt as metal precursor and Phthalic Acid as organic linker (Co-PA) shows distribution of particles as clusters of irregular shaped flower like flakes. SEM image of Mg-PA shows very few pores, at higher magnification little pores space can be identified.

4.2. X-Ray Diffraction Analysis (XRD)

X-ray diffraction was used to investigate crystalline properties of synthesized materials. Powder XRD analysis was achieved before the other characterization tests were done. XRD patterns of Ni-Oxalic, CO-Oxalic and Mg-Oxalic MOFs are presented in Figure 2 (a-c) respectively. In the case of Nickel based as synthesized MOF the dominant diffraction peaks are observed at $2\theta = 10.10^{o}$, 15°, 21.15^{o}, 22.12^{o}, 36°, and 36.5^{o}.

The experimental patterns of Ni-Oxalic MOF are in good agreement with that of nickel (II) benzene tricarbOxalicylate $Ni_3(BTC)_2.12H_2O$ (MOF-Ni) prepared by Wu Jin-ping et.al. Diffraction due to -COOH is detected at lower angels (10.10^o and 15° representing existence of two or three groups attached to the Oxalicalic acid. Presence of small peaks at 15°, and 22.12^o, may be because of the preferred acclimatization of powder sample as similar argument was given by Wu Jin-ping. Normally nickel based MOFs don't show any characteristic peak at higher angles. In present case, existence of peaks at 36.5^o and latter may be the indication of unreacted NiO [13,41,43,71].

High intensity diffraction peak is observed at $2\theta = 44.42^o$ and $2\theta = 64^o$ for cobalt MOF and dominant peaks were observed at $2\theta = 10.5^o$, $2\theta = 21.75^o$, and $2\theta = 34.82^o$ for Magnesium MOF. The patterns of these two MOFs were resembling with Yaghi's MOF-74 and representing crystal structure [72].
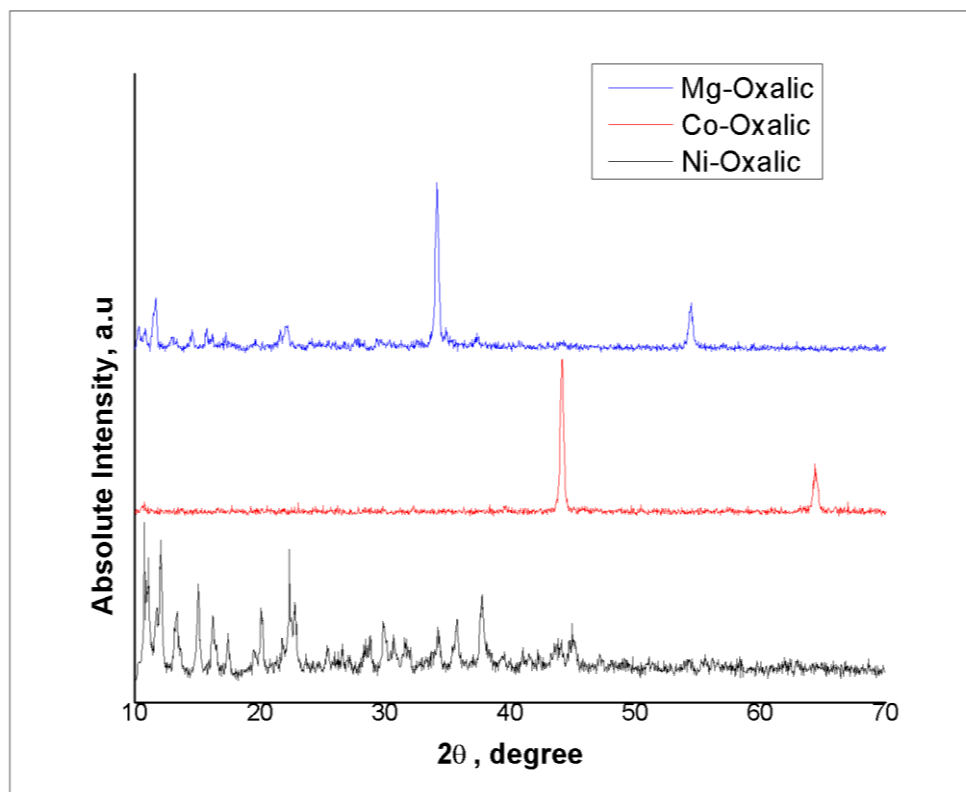

Figure 4. 7 XRD patterns of Oxalic Acid MOFs
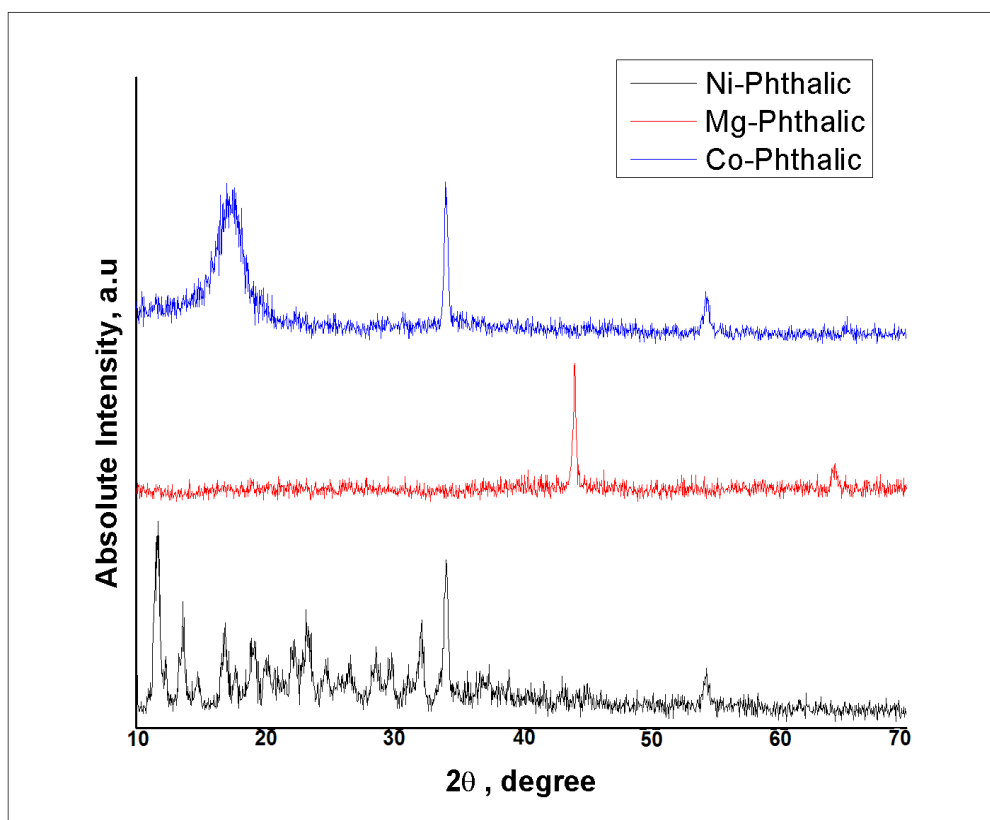
Figure 4. 8 XRD Patterns of Lab Synthesized Phthalic Acid MOFs

In the case of Ni-PA MOF the dominant diffraction peaks are observed at $2\theta = 10.10^{o}$, 12°, 21.15^{o}, 22.12^{o}, 34.5^{o}, and 55°. The experimental patterns of Ni-PA MOF are in good agreement with that of nickel (II) benzene tricarboxylate $Ni_3(BTC)_2.12H_2O$ (MOF-Ni) prepared by Wu Jin-ping et.al. Diffraction due to -COOH is detected at lower angels (10.10^{o} and 15° representing existence of two or three groups attached to the Phthalic acid [67]. Presence of small peaks at 15°, and 22.12^{o}, may be because of the preferred acclimatization of powder sample as similar argument was given by Wu Jin-ping. Normally nickel based MOFs don't show any characteristic peak at higher angles. In present case, existence of peaks at 36° and above may be the indication of unreacted particles.

High intensity diffraction peak is observed at $2\theta = 17.42^{o}$ and $2\theta = 32.5^{o}$ and $2\theta = 54^{o}$ for cobalt MOF and dominant peaks were observed at $2\theta = 44^{o}$, and $2\theta = 64^{o}$ for Magnesium MOF [4,45,73,74].

4.3. Fourier Transform Infra-Red (FTIR)

First, FTIR analysis of pure Oxalic Acid and Phthalic Acid is done by using KBr Technique. Obtained spectra of these pure organic materials are presented in next figures. It is clear from FTIR spectra of MOFs that pure Oxalic and PA have purely different functional group peaks than that of MOFs (after combination of organic part with metal precursor). Peaks of different functional groups at different wavelengths have clearly shown in each spectrum.

First, FTIR analysis of pure Oxalic acid and phthalic acid (organic linkers) was performed as shown in figure 4.9. FTIR spectrum of Oxalic acid observed only three absorbance peaks. The two absorptions band in the region 3450 and 2900 cm^{-1} are representation of O-H and C-H bonds respectively [64].

In Ni-Oxalic FTIR spectra figure are assigned as aromatic C−H stretching vibration originating from the Oxalic acid at 1500 cm^{-1}. The weak and strong bands at 1669 and 1567 cm-1 respectively are assigned as residues of C=O stretching vibration originating from the carbonyl C=O of the Oxalic acid and C−C skeletal vibration of the carboxylic group. The strong band centered at 1392 cm^{-1} corresponds to the C−O stretching vibration. The bands at 500 to 850 cm^{-1} are assigned as ringing- and-out-of-plane bending vibrations of the aromatic ring.
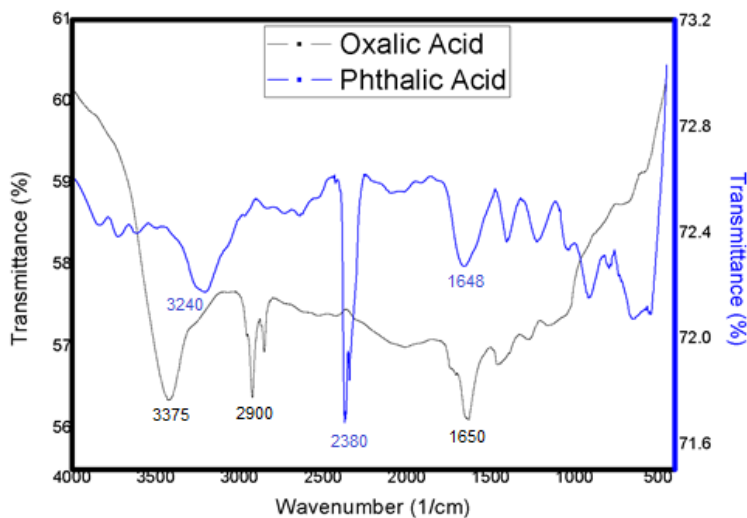

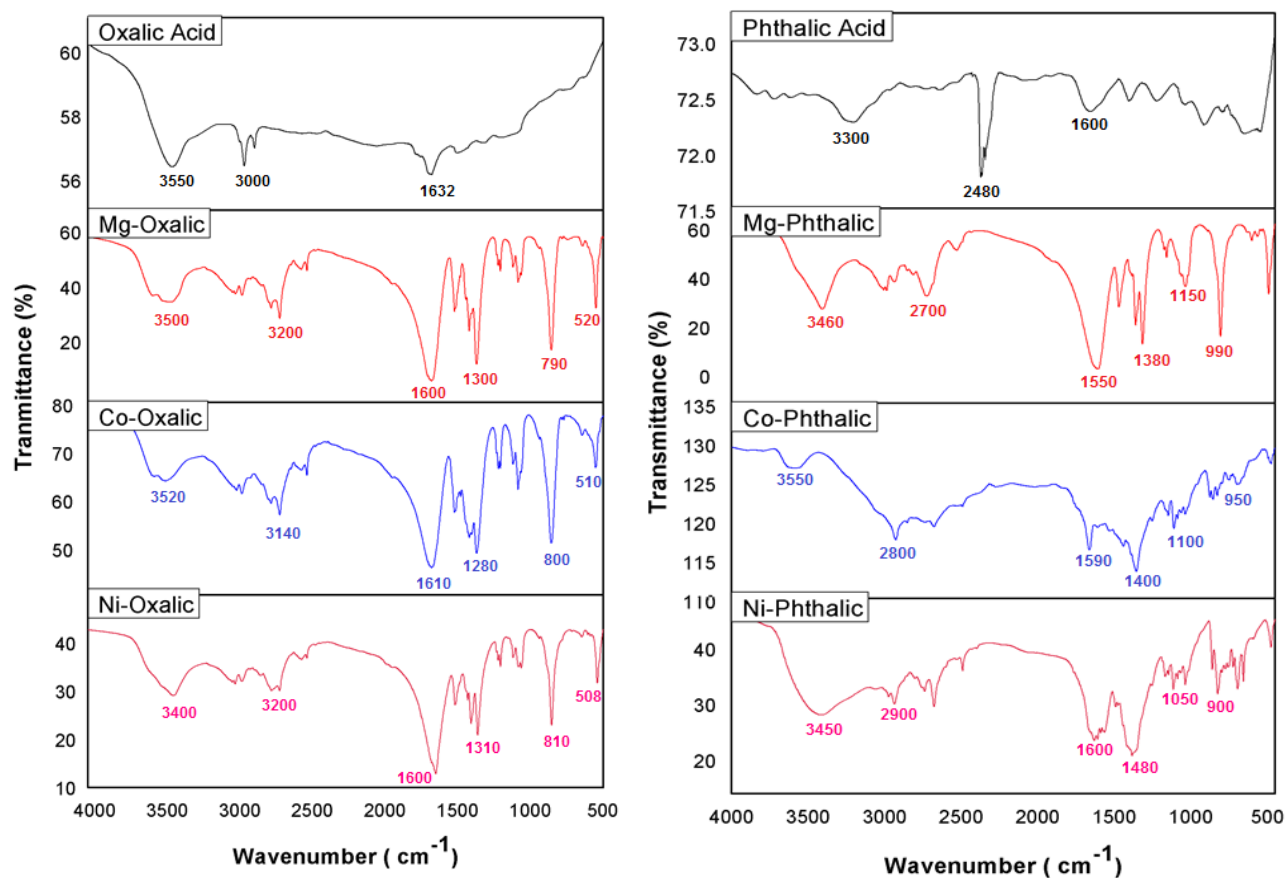**Figure 4. 9 FTIR Spectra of Oxalic Acid and Phthalic Acid**

Figure 4. 10 FTIR Spectra of (a) Oxalic Acid MOFs and (b) Phthalic Acid MOFs

Moreover, the absorption bands seeming in the region 827 to 1350 cm^{-1} can be assigned to the O−C=O symmetric and asymmetric stretching vibrations and the C−O stretching vibration of unreacted Oxalic acid and reacted form of the acid. In the case Mg-Oxalic and Co-Oxalic MOFs show two weak absorption bands in the region 3606 and 3546 cm^{-1} which are assigned as aromatic C−H stretching vibration of the Oxalic acid.

FTIR analysis of pure Phthalic acid (organic linker) was performed and observed the absorption band in the region 2380 cm^{-1} is the representation of C-H bond of aromatic ring. In the IR spectra, the strong and broad bands (O−H stretching vibration) in the 3500-3000 cm^{-1} region indicate the presence of Aromatic C-H Stretching. In the case of Ni-PA MOF, COO appears strong peaks at 1631 and 1383 cm^{-1} and Carboxylic Acid O-H Stretching appears near 2900 cm^{-1}. At 1606 cm^{-1} in Mg-PA MOF COO appears medium intensity peaks and 1660 & 1355 cm^{-1} in Co-PA. 1343 and 1520 cm^{-1} are attributed for NO$_2$ and C=N, respectively. In addition, the strong peaks at 800-850 cm^{-1} reveal presence of Aromatic C-H Bending [75].

4.4. Thermogravimetric Analysis

To investigate the thermal stability and to quantify the weight loss of synthesized MOFs, TGA analysis was achieved and the plot of weight loss % versus temperature is shown in figure 4.11. A controlled temperature program in a controlled atmosphere is given to sample. In simple words, weight loss or gain of a sample specimen with increase and decrease in temperature is measured.

TGA curve for Ni-Oxalic MOF indicating two step weight loss. First one is due to the removal of water in 180-210 °C temperature range. The second weight loss occur in the range of 260-295 °C due to decomposition of carbon ligand. However, after 300 °C no loss in weight was noticed showing the stable structure which is similar to that of early reported Ni based MOF [62,69].
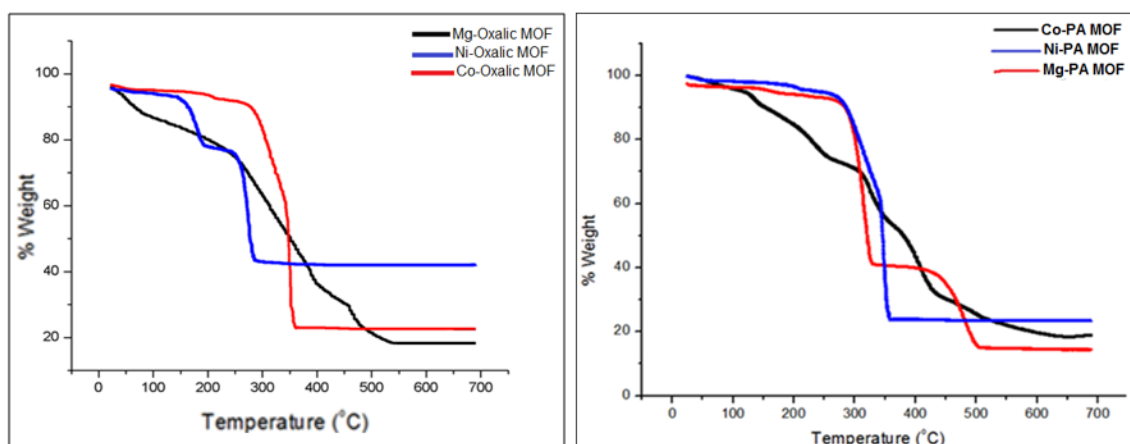
Figure 4. 11 TGA Curves of Phthalic Acid MOFs (a) Oxalic Acid MOFs (b) Phthalic Acid MOFs
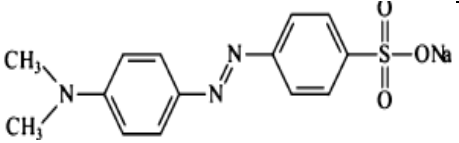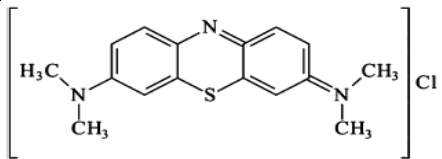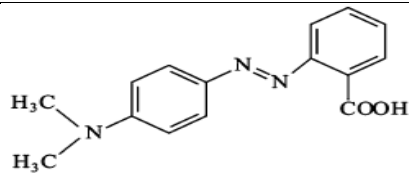
TGA curve for Ni-PA Metallic Organic Framework (MOF) indicating stepwise weight loss. First one is due to the removal of water in 180-210 °C temperature range. The second weight loss occur in between 310-350 °C due to carbon ligand decomposition. After 550 °C no loss in weight was observed confirming the stable MOF structure which is quite similar to that of early reported Ni based MOF [13,70]. For Co-PA and Mg-PA MOFs maximum weight loss occurs at 350°C and 340°C respectively [76].

4.5. Adsorption Experiments

Three stocks solutions of 1000 mg/L of Methyl Orange (MO), Methylene Blue (MB) and Methylene Red (MR) were prepared. The solid organic dyes were dissolved in distilled water to form the solution. To calculate the final concentration of dye after adsorption in different intervals of time, calibration curves were constructed. For this purpose, different concentrations of MO, MB and MR aqueous solution were made through dilution of stock solutions with distilled water as shown in Figure 9.

The pH of these solutions was tested by using HACH Multimeter model: Sension 156, before and after the experiments. No prominent changes in pH values were observed. All adsorbents were dried at 120°C for four hours prior to adsorption. To initiate the experiments, 5mg of each MOF sample was put in 50 mL of fixed initial dye concentration of 5 ppm at 30°C $\pm$ 2 ^{o}C.

Table 4. 1 The chemical structure and nature of organic dyes

Dye	Chemical Structure	Nature	Maximum Absorbance λ_{max} (nm)
Methyl Orange (MO)		Anionic	465
Methylene Blue (MB)		Cationic	668
Methyl Red (MR)		Cationic	436
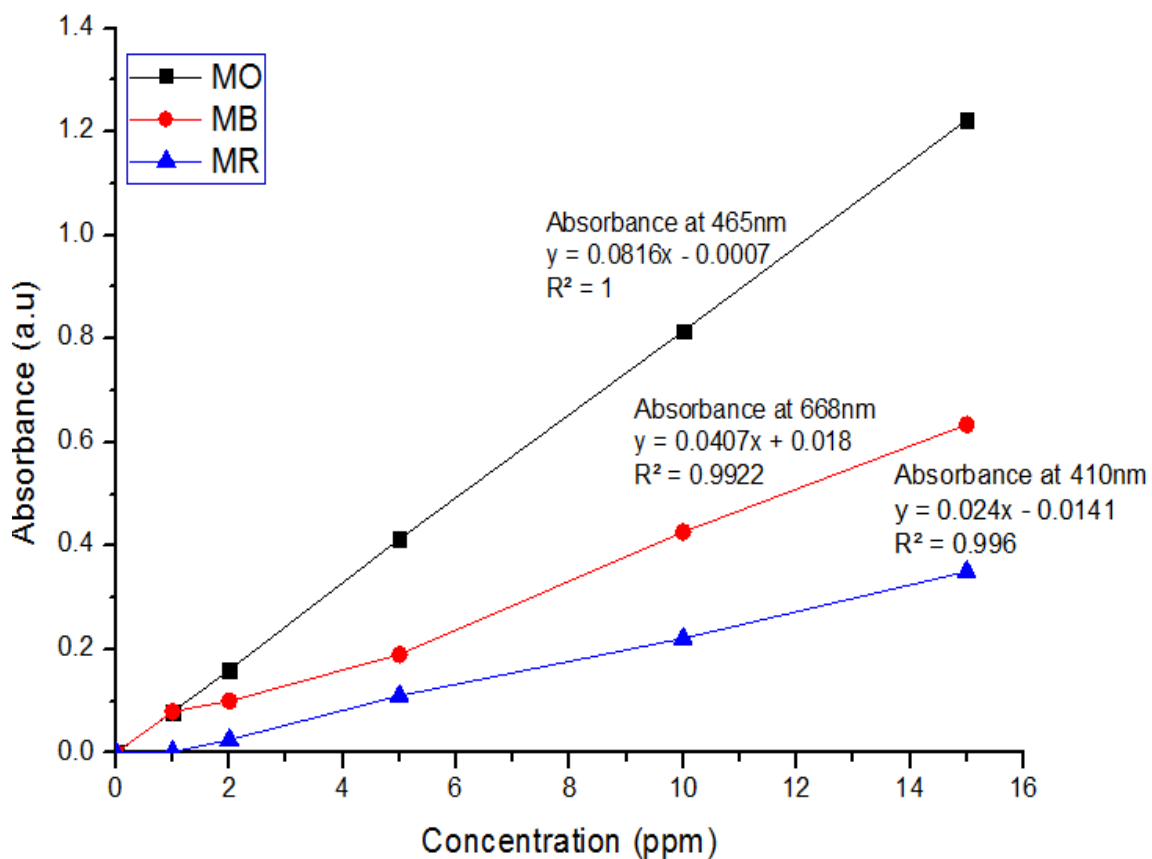
Figure 4.12 Calibration curves and equations for Dye solutions

After adsorption under magnetic stirring at 300 rpm and at different intervals of time the aqueous solutions were separated from MOFs (adsorbents) by filtration. The solutions were analyzed to check the absorbance of dyes on the surface of adsorbents at calibrated maximum wavelengths. Percentage removal of organic dye from aqueous solution was calculated by using following formula:

$$\% \ Removal = \frac{initial \ dye \ concentration - final \ dye \ concentration}{initial \ dye \ concentration} \times 100$$

The equilibrium adsorption capacity (Q_e) was calculated by using following formula:

$$Q_e = \frac{(C_i - C_e) \times V}{m}$$

Where, C_o and C_e represent initial and final concentrations of organic dye (mg/L) of the solution in each experiment.

V = volume of the MOF solution in liters

m = mass of adsorbent in each beaker in grams
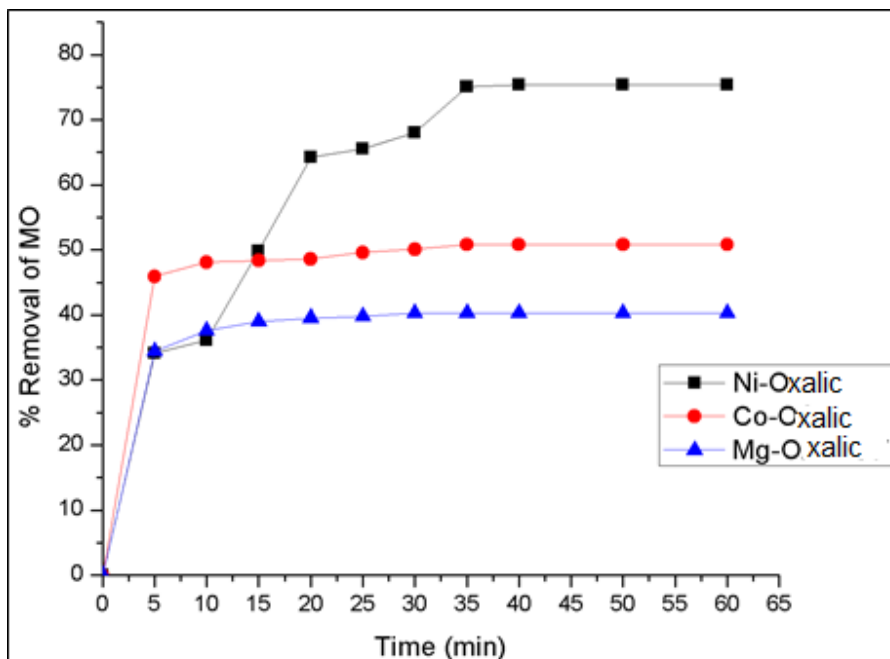
Figure 4.13 Percentage Removal of Methyl Orange with time via Oxalic acid MOFs

In this figure, it is crystal clear that at the start there is a sharp increase in removal (adsorption) of Methyl Orange dye due to availability of vacant sites of adsorbent (MOFs)but after 15 minutes the behavior is changed. Maximum removal is achieved at 35 minutes in the case of Ni-Oxalic MOF.

Figure 4.14 Percentage Removal of Methylene Blue with time via Oxalic Acid MOFs
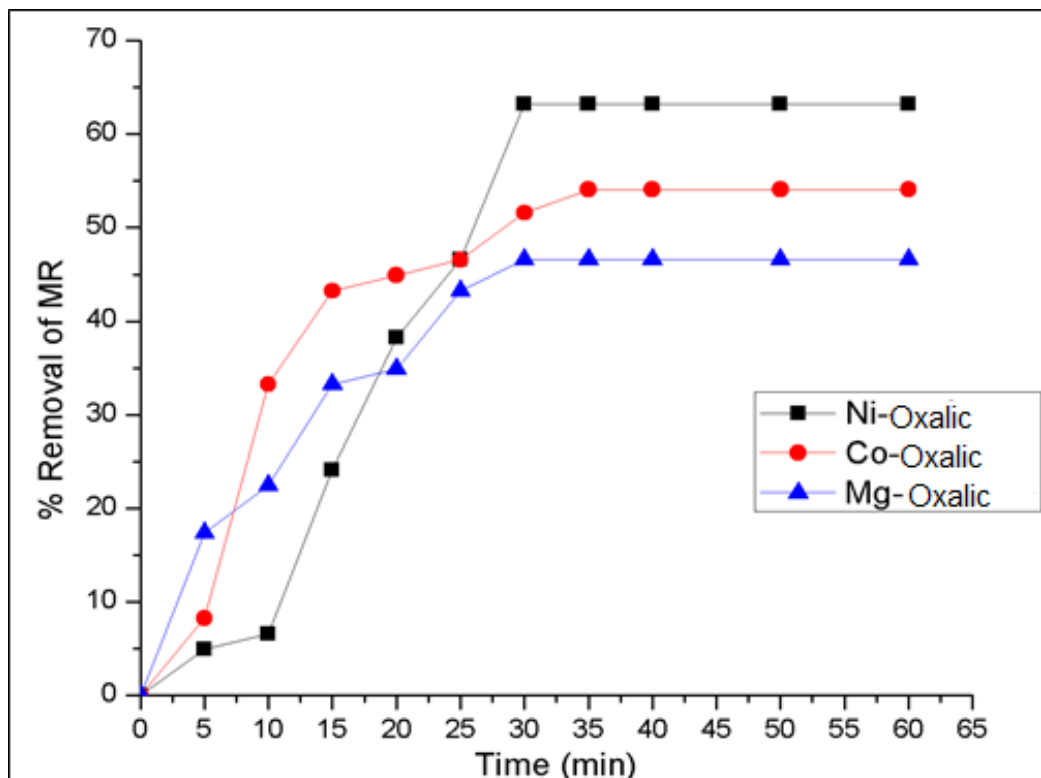
Figure 4.15 Percentage Removal of Methyl Red with time via Oxalic acid MOFs

Similar interaction between adsorbent and adsorbate is experienced for Methylene Blue and Methyl Red as that for Methyl Orange, shown in figure 4.14. Ni-Oxalic MOF shows maximum removal in the start of operation for methylene blue but have very low removal capacity for methyl red in 1st five minutes. As time passes, the interaction of organic dyes with MOFs have different behavior it is due to random cationic- cationic repulsions. Co-Oxalic MOF shows better adsorption of Methyl Red in the start due to presence of plentiful binding sites, but as time increases no exponent removal could be found. For the case of Methylene Blue, both Co-Oxalic and Mg-Oxalic MOFs shows almost similar performance toward percentage removal. The equilibrium time for all three organic dyes was between 30-40 minutes.

Influence of contact time on percentage removal of organic dyes (MO, MB and MR) with the help of lab synthesized Phthalic Acid MOFs is shown in following figures.

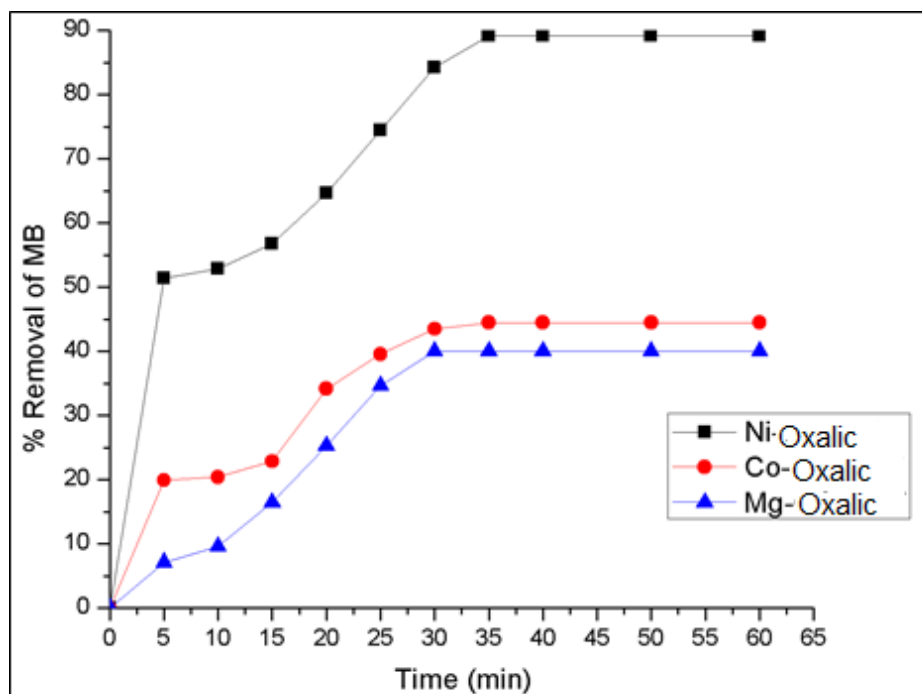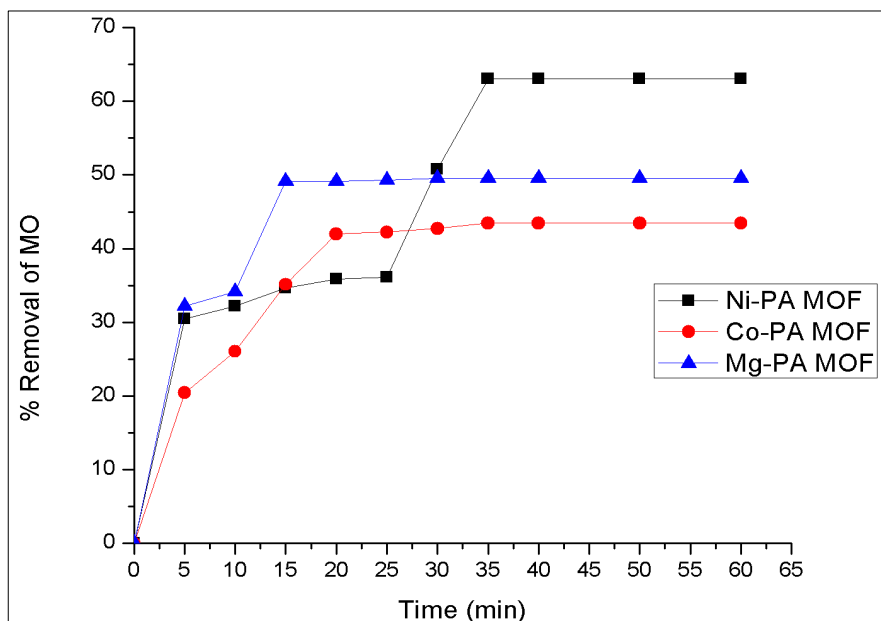**Figure 4. 16 Percentage Removal of Methyl Orange with time via Phthalic Acid MOFs**
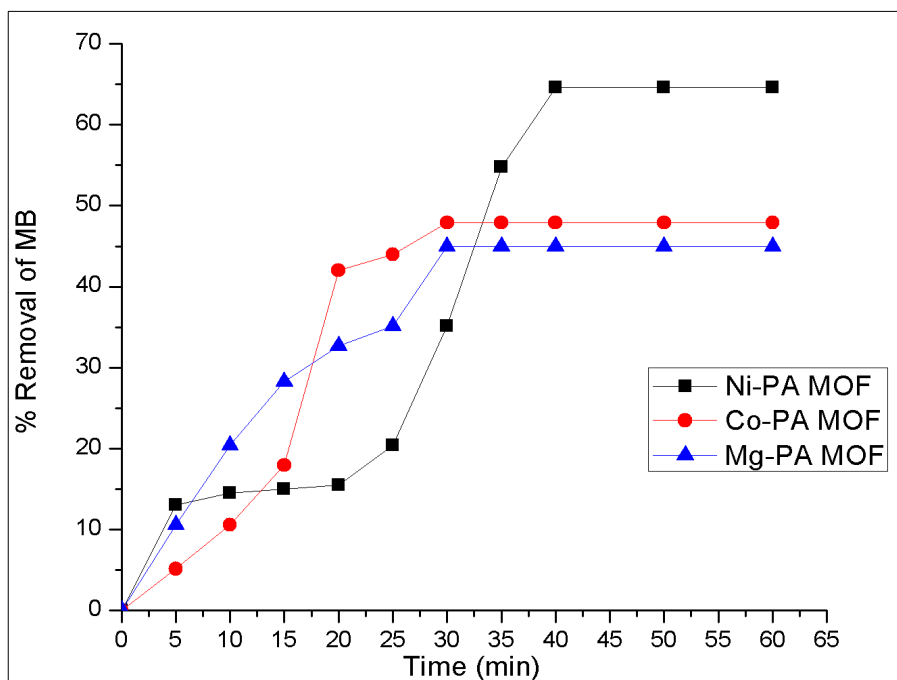
Figure 4.17 Percentage Removal of Methylene Blue with time via Phthalic Acid MOFs
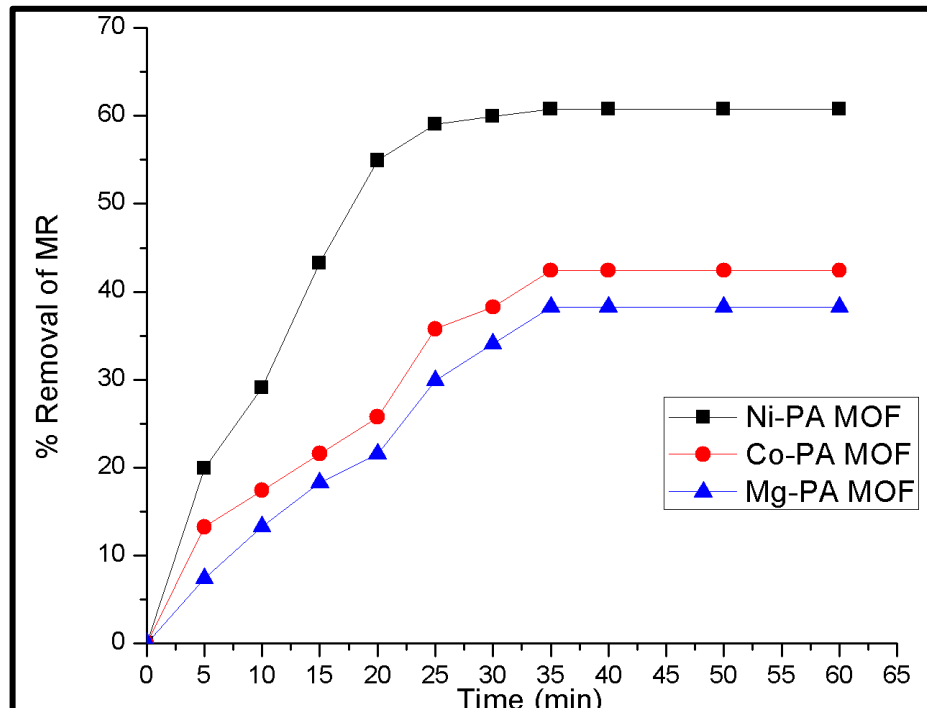
Figure 4.18 Percentage Removal of Methyl Red with time via Phthalic Acid MOFs

Effect of contact time was studied to found equilibrium between adsorbent (MOFs) and Adsorbate (Dyes). For this purpose, the Dye-MOF solution was analyzed by UV spectroscopy to check the absorbance value after different intervals of time. Most of the results revealed the regular rise in percentage removal of dyes upto 10-12 minutes and after that there was decrease in removal due to unavailability of vacant sites of adsorbent and due to desorption phenomena.

Maximum removal of any dye via Phthalic Acid MOFs was 65% which is lower than that of Oxalic Acid MOFs, may be a result of ionic interaction and hindrance. Adsorption removal of Methyl Orange by Mg-PA MOF with relation to contact time gave constant trend after 1st fifteen minutes. There was an irregular fashion for the accomplishment of equilibrium in the case of MB removal for all three MOFs. Approximate direct relation between percentage removal and contact time was experienced for adsorptive removal of Methyl Red via Phthalic acid MOFs and for batch experiments the equilibrium time was between 30-35 minutes.

4.6. Adsorption Isotherm

Different Isotherms are used to know how molecules allocate themselves between liquid and solid phases at equilibrium. The interaction of adsorbates with adsorbents is described with the help of these adsorption isotherms. Langmuir model and Freundlich isotherm models are the most common adsorption models [77].

4.6.1. Langmuir Isotherm

Langmuir adsorption model supposes that maximum adsorption takes place at a monolayer of solute molecules on the surface of adsorbent. This isotherm has been exercised in many monolayer adsorption processes. Linearized form of the Langmuir adsorption can be written by using following equation:

$$\frac{C_e}{Q_e} = \frac{1}{Q_m K_L} + \frac{C_e}{Q_m} \ [78]$$

Where Q_e in mg/g expresses the equilibrium adsorption capacity of the MOF, C_e is the equilibrium dye concentration in solution (mg/L), Q_{max} is the maximum amount of dye that could be adsorbed on the adsorbent and K_L in L/mg shows the Langmuir adsorption equilibrium constant.

The Langmuir equation can also be stated in terms of a dimensionless separation factor R_L, for guessing the favorability of an adsorption system, defined as follows:

$$R_L = \frac{1}{1 + C_m \ K_L} \ [79]$$

In general, If $R_L<1$, then the adsorption is favorable, If $R_L=0$, then the adsorption attribute is irreversible, If $R_L=1$, then the adsorption characteristic is linear, If $R_L>1$, then the adsorption is unfavorable. Correlation coefficient (R^2 is used to know the applicability of the isotherm models to the adsorption behavior [79].

From graph of Ce and Ce/Qe, maximum adsorption capacity, adsorption equilibrium constant and dimensionless separation factors are calculated. **Slope = 1/Q$_m$; y-intercept = 1/Q$_m$.K$_L$** All the calculated values are listed in table 4.2 and 4.3.

4.6.2. Freundlich Isotherm

The Freundlich isotherm model is an empirical association explaining the adsorption of solutes particles from a liquid phase to a solid surface and assumes that different sites with several adsorption energies are concerned. Affiliation between the amounts of dye adsorbed per unit mass of adsorbent is clearly described by Freundlich adsorption isotherm. The linear form of Freundlich isotherm model can be expressed by following equation:

$$\ln Q_e = \ln K_F + \left(\frac{1}{n}\right) \ln C_e \quad [80]$$

where K_F and n are the Freundlich constants, the properties of the system. K_F and n are the pointers of the adsorption capacity and adsorption intensity, respectively.

The aptitude of Freundlich model to fit the experimental data was inspected. For this case, the plot of log Ce vs. log qe was used to make the intercept value of K_F and the slope of n. The magnitudes of K_F and n show easy from the aqueous solution and indicate favorable adsorption. The intercept K_f value is an indication of the adsorption capacity of the adsorbent; the slope $1/n$ shows the effect of concentration on the adsorption capacity and represents adsorption intensity.

Large K_F value shows that adsorption is greater however, when value for $n_F = 1$, the adsorption is linear. For $n_F < 1$ the type of adsorption is lies in the region of chemisorption, and for $n_F > 1$, the adsorption favors the physical process. $K_F = \ln$ of maximum Qe, Slope = 1/n.

It can be seen from table 4.2 that for adsorption of Methyl Orange dye from water using Ni-Oxalic, Co-Oxalic and Mg-Oxalic, the value of 1/n is 0.76, 1.05 and 1.67 respectively. So, it is concluded that Ni-Oxalic has shown chemisorption while Co-Oxalic and Mg-Oxalic has indicated physic-sorption nature.

Table 4. 2 Adsorption isotherm models constants for the Oxalic Acid MOF Samples

| Organic Pollutants | Adsorbent (MOF) | Langmuir and Freundlich Isotherm Constants | | | | | | |
| | | Langmuir Isotherm | | | | Freundlich Isotherm | | |
		K_L (L/mg)	Q_m (mg/g)	R^2	R_L	K_F (mg/g)	1/n	R^2
Methyl Orange	Ni-Oxalic	41.00	24.39	0.988	0.004	3.62858	0.76	0.854
	Co-Oxalic	1.61	16.13	0.907	0.110	3.234923	1.05	0.899
	Mg-Oxalic	1.25	12.33	0.677	0.138	3.00245	1.67	0.898
Methylene Blue	Ni-Oxalic	4.42	25.13	0.978	0.042	3.797613	0.34	0.955
	Co-Oxalic	1.03	10.15	0.702	0.163	3.101707	2.14	0.958
	Mg-Oxalic	0.61	4.32	0.509	0.247	2.99696	3.47	0.948
Methyl Red	Ni-Oxalic	0.71	2.77	0.931	0.221	3.517745	2.07	0.873
	Co-Oxalic	0.62	4.76	0.539	0.244	3.297379	2.46	0.897
	Mg-Oxalic	0.95	10.06	0.659	0.174	3.148096	2.06	0.969

As Large K_F value point toward greater adsorption capacity, maximum value is obtained for Ni-Oxalic MOF toward removal of Methylene Blue. For all cases R_L is less than one, so adsorption characteristic is favorable. As shown in the table 4.2, it was clear that correlation coefficient (R^2) fitted to the Langmuir model was higher than that of Freundlich model.

Table 4. 3 Adsorption isotherm models constants for the Phthalic Acid MOF Samples

| Organic Pollutants | Adsorbent (MOF) | Langmuir and Freundlich Isotherm Constants | | | | | | |
| | | Langmuir Isotherm | | | | Freundlich Isotherm | | |
		K_L (L/mg)	Q_m (mg/g)	R^2	R_L	K_F (mg/g)	1/n	R^2
Methyl Orange	Ni-PA	21.71	19.19	0.971	0.009	3.450999	1.08	0.986
	Co-PA	1.45	14.29	0.890	0.121	3.078599	2.09	0.986
	Mg-PA	2.13	17.83	0.815	0.086	3.210508	1.43	0.993
Methylene Blue	Ni-PA	0.88	6.12	0.834	0.185	3.475364	1.67	0.951
	Co-PA	0.57	3.21	0.528	0.259	3.176209	3.11	0.935
	Mg-PA	0.72	6.89	0.526	0.217	3.112696	2.75	0.925
Methyl Red	Ni-PA	0.96	10.41	0.763	0.172	3.41362	1.41	0.960
	Co-PA	0.85	7.84	0.616	0.190	3.054394	2.56	0.967
	Mg-PA	0.66	5.18	0.459	0.232	2.950996	3.45	0.932

Maximum Kf value was for the case of methylene blue adsorption on to the Ni-PA MOF. For the same case correlation coefficient (R^2) fitted to the Freundlich model was higher than that of Langmuir model. 1/n value for Ni-Oxalic MOF was below one, indicates the adsorption follow Langmuir isotherm model.

4.7. Kinetic Study

Chemical kinetics is an investigation of rates of chemical processes and factors that effect in the accomplishment of equilibrium in a logical amount of time. It also gives indications on the mechanism of the adsorption process as well as an estimation of the loading of the adsorbent at equilibrium capacity. Lagergren pseudo first-order and Lagergren pseudo-second-order are the most common kinetic models. The pseudo first order kinetic model can be represented as linear form by following equation:

$$ln(Q_e - Q_t) = ln\ Q_e - k_1 t\ [24]$$

The Pseudo Second order model can be expressed as linear form by:

$$\frac{t}{Q_t} = \frac{1}{K_2 Q_e{}^2} + \frac{t}{Q_e}\ [77]$$

Where Qe and Qt are the amount of adsorbate (dye) on the surface of adsorbent (MOFs) in mg/g at the equilibrium and time t (min), respectively [81].

For many adsorption practices, the pseudo-first-order kinetics was realized to be appropriate for only the initial 20 to 30 minutes of interaction time and not for the whole span of contact times. In addition, it was found that k1 alters with the initial concentration of the adsorbate and varies considerably depending on the adsorption system. To take in mind these points, pseudo second order equation is applied to model the kinetics of organic dye adsorption onto lab prepared MOFs.

In pseudo 2nd order kinetic model K2 (g/mg.min) represents the pseudo second-order rate constant. If the adsorption system follows a pseudo-second-order kinetics the main assumption being that the rate limiting step may be chemical adsorption involving valence forces through sharing or the exchange of electrons between the adsorbent and the metal ions then a plot of t / Qt (min.g/mg) versus t (min) would be linear and values of K_2 and R^2 can be revealed from the graph. One of the main pros of the pseudo-second-order equation for estimating Qe values is its small sensitivity to the influence of casual experimental errors.
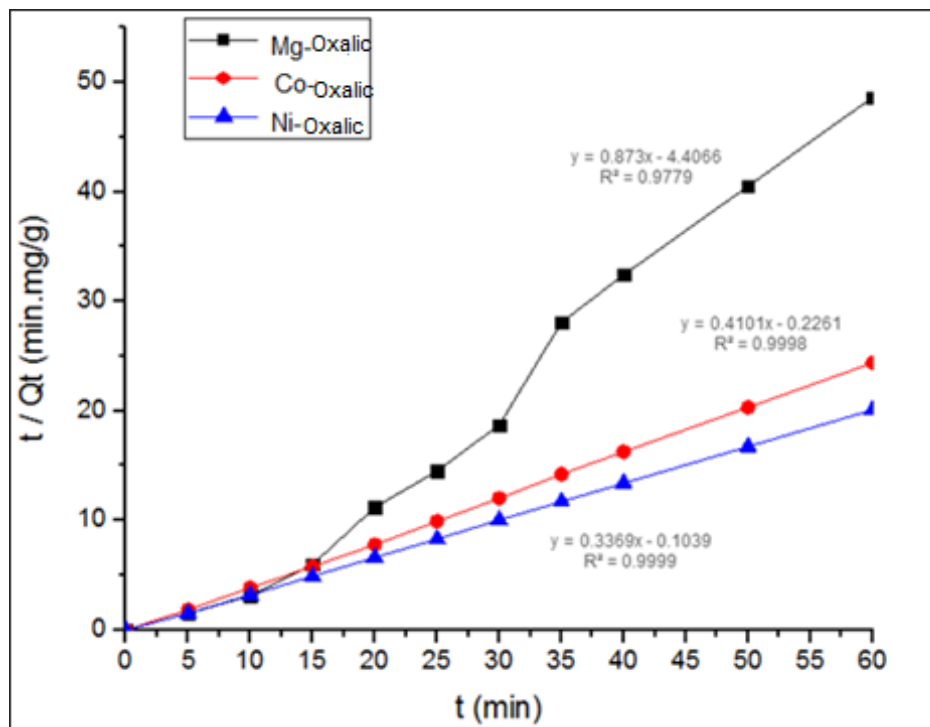
Figure 4. 12 Plot of pseudo 2nd order kinetic model for MO adsorption of Oxalic Acid MOFs

Per data shown in graphs, the adsorption of organic dye on Ni-Oxalic and Ni-PA MOFs followed pseudo second-order kinetics because of the favorably fit between experimental and calculated values of Qe (R^2 values above 0.99). So, Ni-MOF adsorption of MB is a chemical adsorption.

Figure 4. 13 Plot of pseudo 2nd order kinetic model for MB adsorption of Oxalic Acid MOFs

Figure 4. 14 Plot of pseudo 2nd order kinetic model for MR adsorption of Oxalic Acid MOFs

Figure 4. 15 Plot of pseudo 2nd order kinetic model for MO adsorption of Phthalic Acid MOFs

The adsorption kinetics was applied to the batch experiments for removal of three organic dyes. Kinetic data is used to check the rate at which dyes are removed from the solution. Figure 4.23-4.25 show kinetic equation and constant for adsorption of dyes via Phthalic Acid MOFs. The graphs indicate these MOFs follow Pseudo 2nd order kinetics because of favorably fir R^2 value (above 0.9).
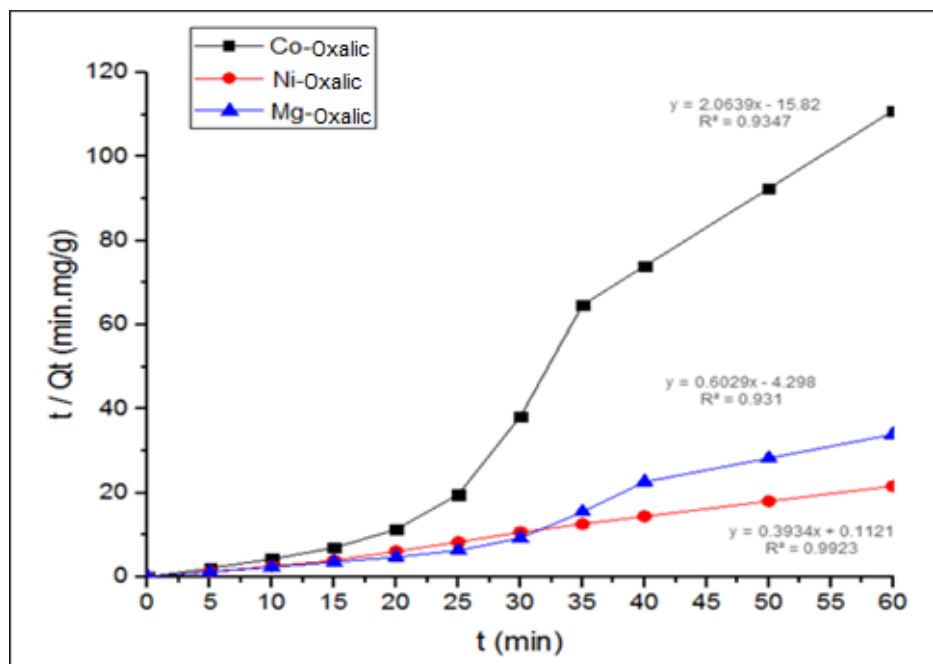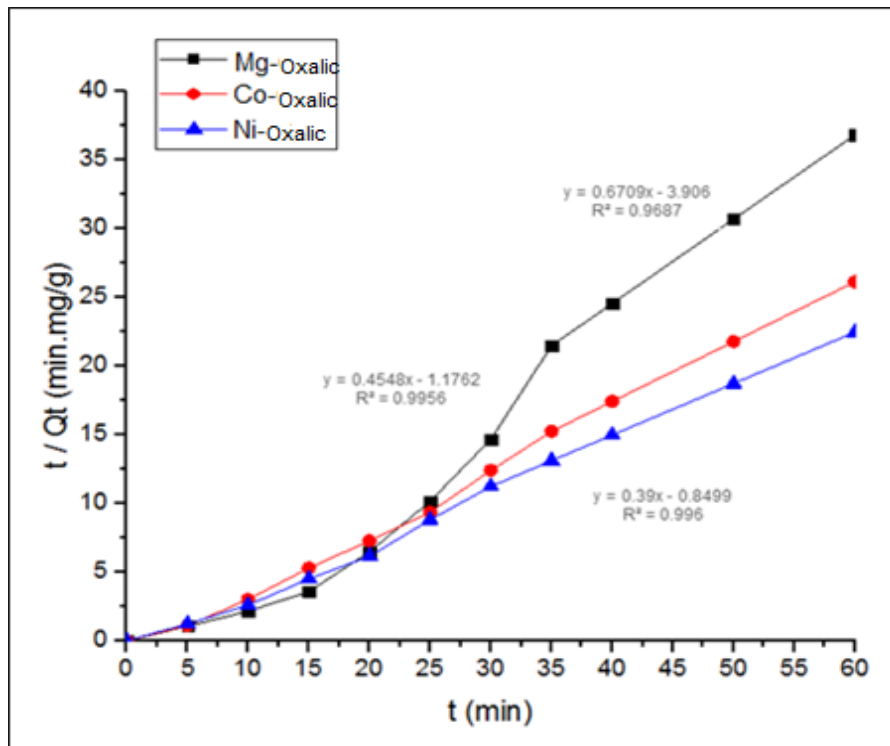

Figure 4. 24 Plot of pseudo 2nd order kinetic model for MB adsorption of Phthalic Acid MOFs

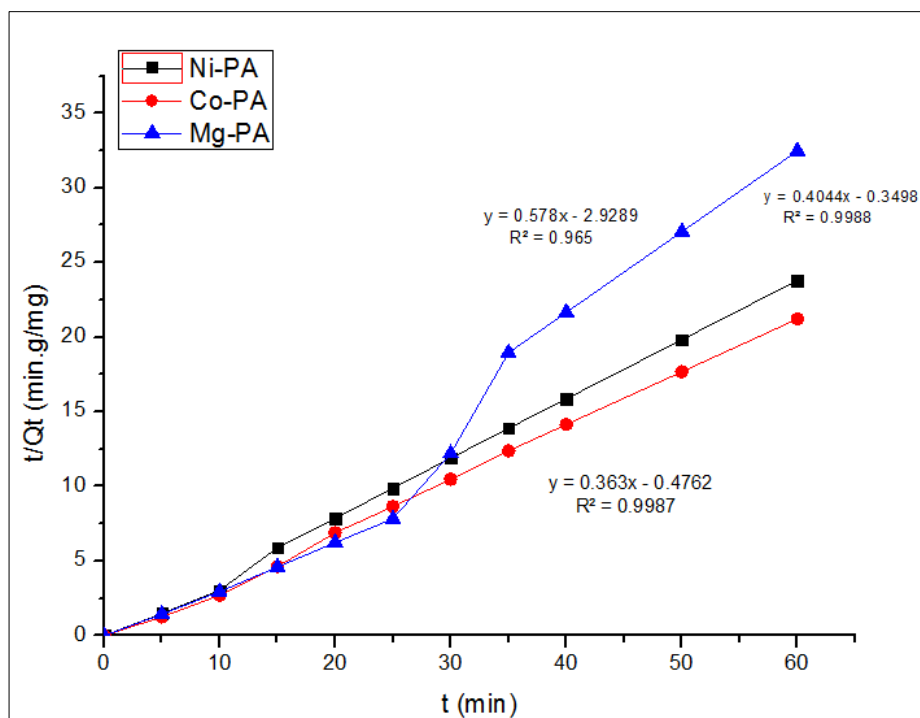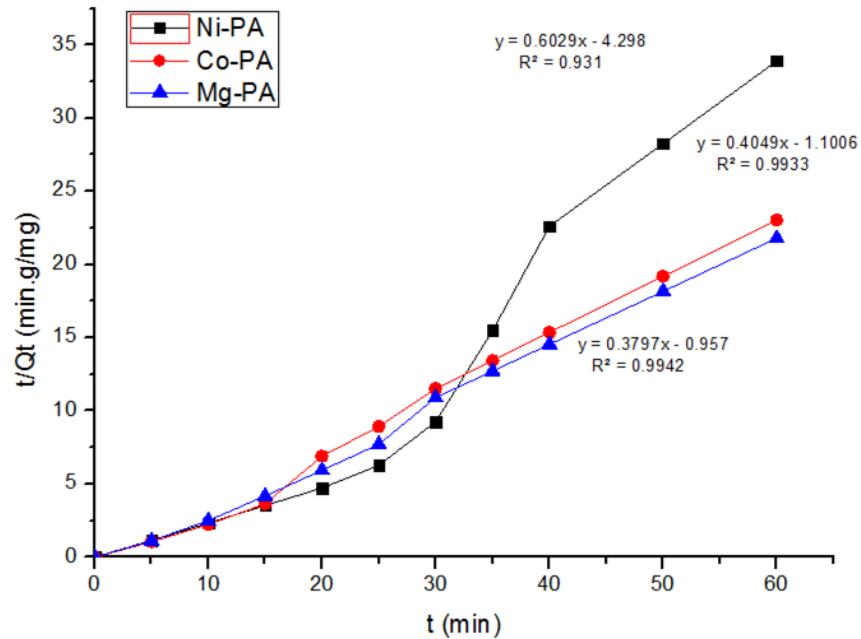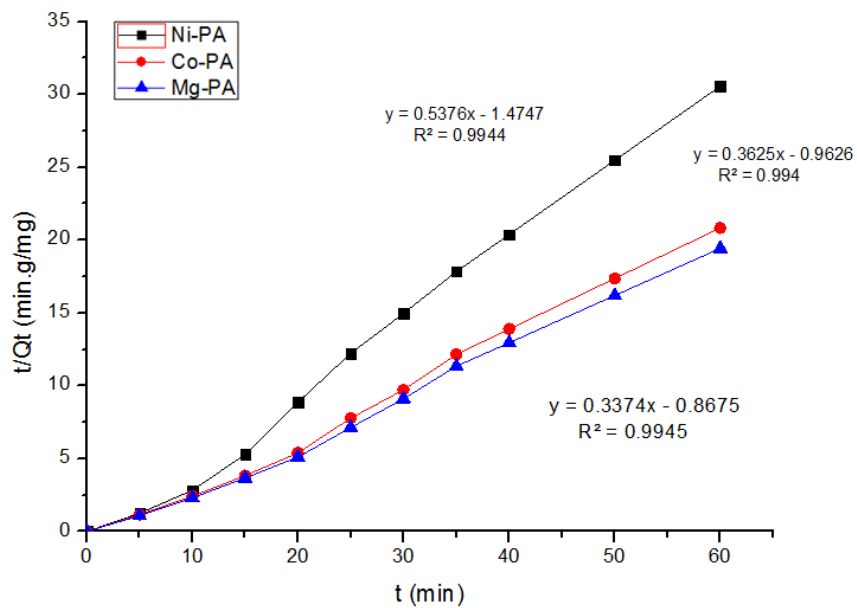**Figure 4. 25 Plot of pseudo 2nd order kinetic model for MR adsorption of Phthalic Acid MOFs**

4.8. Efficiency of Lab Prepared MOFs

Figure 4.26 clearly indicates that maximum removal of organic dyes was achieved with the help of Ni-Oxalic MOFs. Almost 90 % adsorptive removal of Methylene Blue and 86 % of Methyl Orange was found. Minimum percentage removal was gained of methyl orange via Mg-Oxalic MOF. For all three dyes, Mg-Oxalic MOFs could adsorb minimum quantity of adsorbates, as SEM, XRD results indicated for this MOF. After Ni-Oxalic MOF better results were got via Co-Oxalic Acid MOF i.e. almost 65 % removal of Methyl Red after one hour adsorbent-adsorbate interaction.
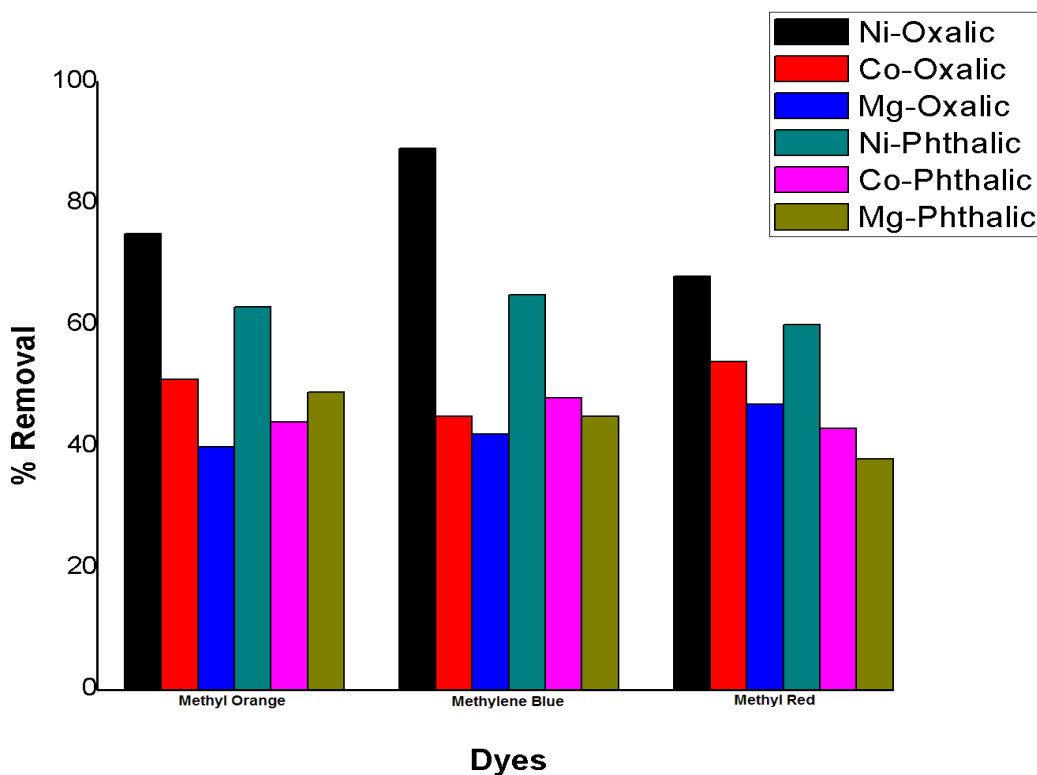
Figure 4.26 Percentage Dyes Removal Efficiency of Lab synthesized MOFs

For the case of Phthalic Acid MOFs, equilibrium was achieved in between 30-35 minutes after this time removal tendency of organic dyes was constant. After one hour batch adsorption experiments, maximum removal of dye was 65 % for the Methylene Blue via Ni-Phthalic Acid MOF. Naturally, MB as a cationic dye can be adsorbed by Ni-MOFs because of electrostatic forces of interaction. Minimum percentage of organic dye was found to be for Methyl Red with Mg-MOF. Interestingly, Mg-PA MOF shows higher removal of Methyl Orange than that of Co-PA MOF, may be this behavior was due to the presence of cohesive force between anionic MO dye and adsorbent surface.

Conclusions and Recommendations

5.1. Conclusions

Six Metal Organic Frameworks (MOFs) have been synthesized in present work by using inexpensive metal salts of nickel, cobalt and magnesium chemically-tailored dicarboxylic acid organic bridging units of oxalic acid and phthalic acid. The combination of these two components in solution at room temperature and under hydrothermal conditions results in the formation of a three-dimensional network solids, which has a very high porosity and surface area as revealed by SEM analysis. SEM images shows that among synthesized series of MOFs, the Ni-Oxalic has highly porous structure. Powder XRD patterns confirm the crystalline structure of these materials. The broadening of hydroxyl peak in arrange of 3000-3500 cm^{-1} for organic linker in FTIR spectra show the incorporation of metal with organic ligand and hence confirm that MOFs has been successfully synthesized. Adsorption study of methyl orange, methylene blue and methyl red dyes on MOF adsorbents was performed by uv-visible spectroscopy in batch process. The nickel-oxalic acid metal organic framework shows best adsorption capacity up to 90% at room temperature for methylene blue dye from aqueous solution, whereas nickel-phthalic acid MOF shows about 60% dye adsorption capacity. In case of methyl orange dye, the nickel-oxalic acid MOF shows high capacity of removal up to 76% whereas nickel phthalic acid shows about 60% dye removal. Similarly for methyl red, the nickel oxalic acid shows 70% adsorption capacity, whereas nickel-phthalic acid adsorb about 60% of the dye from aqueous solution under ambient conditions. The magnesium and cobalt metals MOFS shows adsorption capacity in range of 35-45%. Therefore, generally these materials have potential application for waste water treatment. Kinetic studies of dyes adsorption illustrate that the adsorption process is chemisorption monolayer formation and follow pseudo second order kinetics.

5.2. Future Recommendations

- The regeneration capacity study of these synthesized MOFs can be performed in the future work.

- The synthesized MOF can be incorporated in polymeric membrane to develop mix-MOF-membrane with enhance the gas separation capacity.

- The thermodynamic study for enthalpy or entropy changes associated with dyes adsorption can also be studied.

- The synthesized MOF can be tested for their adsorption capacity for heavy metal removal from waste water.

REFERENCES

[1]   L.R. Macgillivray, *Metal-organic frameworks: design and application*, John-wiley and Sons, London, **2010, 25-35.**

[2]   B. Seyyedi, *Metal-Organic Frameworks : A New Class of Crystalline Porous Materials*, Lambert Academic Publishing, Germany, **2015, 45-50.**

[3]   B. Li, M. Chrzanowski, Y. Zhang, *Applications of metal-organic frameworks featuring multi-functional sites*, Coordination Chemistry Reviews, **2016**, 307, 106-129.

[4]   M. Tunable, R.J. Comito, *Metal Organic Frameworks and Covalent Organic Frameworks*,American Chemical Society, **2006**,115-119.

[5]   Z. Zhao, Z. Li, Y.S. Lin. *Adsorption and Diffusion of Carbon Dioxide on Metal - Organic Framework (MOF-5)*, Industrial & Engineering Chemistry Research, **2009**, 48,10015-10020.

[6]   C. Dey, T. Kundu, B.P. Biswal, A. Mallick, *Crystalline metal-organic frameworks (MOFs): synthesis , structure and function*, Acta Crystallographica Section B, **2014**,70, 3-10.

[7]   K. Omar, E.Christopher, *Designing Higher Surface Area Metal−Organic Frameworks*, J. Am. Chem. Soc., **2012**, 134 (24), 9860–9863.

[8]   B Chen, C Liang, J Yang, DS Contreras, *A microporous metal-organic framework for gas-chromatographic separation of alkanes*, Chem Int Ed Engl. , **2006**, 45(9), 1390-3.

[9]   KS. Walton, RQ. Snurr, *Applicability of the BET Method for Determining Surface Areas of Microporous Metal Organic Frameworks*, J. Am. Chem Soc. **2007**, 129 (27), 8552-6.

[10]   H. Mohideen, *Novel Metal Organic Frameworks : Synthesis , Characterization and Functions*, Andrews Research Repository, **2011**, 75-85.

[11]   M. Eddaoudi, DF. Sava, JF. Eubank, K. Adil, *Zeolite-like metal–organic frameworks (zmofs): design, synthesis, and properties*. Chem Soc Rev, **2015**, 44, 228-249.

[12]   G. Férey. *Hybrid porous solids: past, present, future*. Chem Soc Rev, **2008**, 37,

191-214.

[13]   H.Y. TAN, W. Zhao. Simple Preparation , *Structure and Conductivity of Nickel Benzenetricarboxylate*, Chinese J. Struct. Chem. **2014**, 401─406.

[14]   M. Mohamedali, D. Nath, H. Ibrahim, *Review of Recent Developments in CO2 Capture Using Solid Materials : Metal Organic Frameworks*, Intech science, **2013**, 115-154.

[15]   ST. Meek, JA. Greathouse, MD. Allendorf, *Metal-Organic Frameworks : A Rapidly Growing Class of Versatile Nanoporous Materials*, Adv Mater., **2011**, 23(2), 249-67.

[16]   H. Zeiger. *How metal-organic frameworks could help realize a carbon-neutral energy cycle*, techxplore, **2016**,1-3.

[17]   Dkhil B, Lloret F, Nakagawa K, Tokoro H, Ohkoshi S, Verdaguer M. High Proton *Conduction in a Chiral Ferromagnetic Metal À Organic*, Int. Ed., **2011**, 123, 7266–7269.

[18]   J. Ren, NM. Musyoka, HW. Langmi, BC. North, *A more efficient way to shape metal-organic framework (MOF) powder materials for hydrogen storage applications*, International Journal of Hydrogen Energy, **2015**, 40 (13), 4617-4622.

[19]   M. Sharma, RK. Vyas, K. Singh, *A review on reactive adsorption for potential environmental applications*, Adsorption, **2013**, 19(1), 161-188

[20]   Saqib J, Aljundi IH. *Membrane fouling and modification using surface treatment and layer-by-layer assembly of polyelectrolytes* : State-of-the-art review. Journal of Water Process Engineering, **2016**, 11, 68-87.

[21]   A. Majedi, F. Davar F, AR. Abbasi, *Metal-organic framework materials as nano photocatalyst*, International Journal of nano dimension, , **2016**, 7 (1), 1-14.

[22]   Y. Ide, N. Kagawa, M. Sadakane M, *Sunlight-induced effective heterogeneous photocatalytic decomposition of aqueous organic pollutants to CO2 assisted by a CO2 sorbent, amine-containing mesoporous silica*. Chemical Communications, **2012**, 44, 5521-5523.

[23]   G. Yu, M. Xue, Z. Zhang, J. Li , *A water-soluble pillararene: Synthesis, host-guest chemistry, and its application in dispersion of multiwalled carbon*

nanotubes in water. J. Am. Chem. Soc., **2012**, 134 (32), 13248–13251.

[24] FJ. Beltran, V. Gmez-Serrano, A. Durn, *Degradation kinetics of p-nitrophenol ozonation in water*. Water Research, **1992**, 26, 9–17

[25] Z. Yang ,YC. Juang, DJ. Lee, *Pore blockage of organic fouling layer with highly heterogeneous structure in membrane filtration: Role of minor organic foulants*, Journal of Membrane Science, **2012**,3, 5-12.

[26] M. Nurisepehr, S. Jorfi, R. Kalantary, H. Akbari, Samaei M. *Sequencing treatment of landfill leachate using ammonia stripping, Fenton oxidation and biological treatment*. Waste Management & Research : The Journal of the International Solid Wastes and Public Cleansing Association, **2012**, 12, 25-35

[27] Y. Kato, M. Machida, H. Tatsumoto, *Inhibition of nitrobenzene adsorption by water cluster formation at acidic oxygen functional groups on activated carbon.* Journal of Colloid and Interface Science, **2008**,7,11-18.

[28] J. Lu,T. Zhang, J. Ma, Z. Chen, *Evaluation of disinfection by-products formation during chlorination and chloramination of dissolved natural organic matter fractions isolated from a filtered river water*. Journal of Hazardous Materials, **2009**,3,27-34.

[29] MN. Chong, B.Jin, C. Saint, *Recent developments in photocatalytic water treatment technology*: A review. Water Research, **2010**, 44 (10), 2997-3027.

[30] H. Yang, H. Cheng, *Controlling nitrite level in drinking water by chlorination and chloramination.* Separation and Purification Technology, **2007**, 56, 392–396.

[31] Z. Hasan, SH. Jhung,. Journal of Hazardous Materials, **2014**, 244-245, 444-456.

[32] L. Öhrström, *Topology and Terminology of Metal-Organic Frameworks and Why We Need Them*. Crystals, **2015**, 5(1), 154-162.

[33] N. Stock N, S. Biswas, *Synthesis of Metal-Organic Frameworks*, **2012**, Chem. Rev.,112 (2), 933–969.

[34] SR. Batten, NR. Champness, S.Kitagawa, *Coordination polymers, metal–organic frameworks and the need for terminology guidelines*. Crystengcomm, **2012**, 9,332-341.

[35] LR. Macgillivray, *Metal Organic Frameworks -Design and Application.*, Chem. Commun., **2012**, 48, 7958-7960.

[36] R. Seetharaj, P. Vandana, P. Arya, S. Mathew, *Dependence of solvents , ph , molar ratio and temperature in tuning metal organic framework architecture*. Arabian journal of chemistry, **2016**,5, 35-42.

[37] JS. Lee, SB. Halligudi, NH. Jang, *Microwave Synthesis of a Porous Metal-Organic Framework , Nickel (II) Dihydroxyterephthalate and its Catalytic Properties in Oxidation of Cyclohexene,* Bulletin of the Korean Chemical Society, **2010**, 31(6),1489-1495.

[38] P. Falcaro, R. Ricco, A.Yazdi, *Application of Metal and Metal Oxide Nanoparticles mofs*. Coordination Chemistry Reviews, **2015**, 237-254.

[39] NT. Phan, P.Vu,TT. Nguyen, *Expanding applications of copper-based metal – organic frameworks in catalysis*. Journal of Catalysis, **2013**, 306, 38-46.

[40] G. Crini, *Non-conventional low-cost adsorbents for dye removal:* A review. Bioresource Technology, **2006**, 97 (9), 1061-85.

[41] A. Ayati, MN. Shahrak, B. Tanhaei, *Chemosphere Emerging adsorptive removal of azo dye by metal e organic frameworks*. Chemosphere, **2016**, 160, 30-44.

[42] S. Lin, Z. Song,G. Che,A. Ren, *Adsorption behavior of metal-organic frameworks for methylene blue from aqueous solution*. Microporous and Mesoporous Materials, **2014**,43, 145-156.

[43] S. Mansab,U. Rafique, N. Haq, *Synthesis of Ni based metal organic frameworks and its applications for removal of polyaromatic hydrocarbons, International* Journal of Innovation and Scientific Research **2015**, 15 (2), 443-451.

[44] M. Tong, D. Liu,Q. Yang, *Influence of the framework metal ions on the dye capture behavior of the MIL-100. Experimental and computational details,* The Royal Society of Chemistry, **2013**, 28, 117-127.

[45] J.Yang, *Hydrogen storage in Metal Organic Frameworks,* Chem. Rev., **2012**, 112 (2), 782–835.

[46] HW. Langmi, J. Ren., B. North, M. Mathe, *Electrochimica Acta Hydrogen Storage in Metal-Organic Frameworks* : A Review. Electrochimica Acta, **2017**, 128, 368-392.

[47] E. Volkova, A.V. Vakhrushev, M. Suyetin, *Improved design of metal-organic frameworks for efficient hydrogen storage at ambient temperature : A multiscale*

theoretical investigation. International Journal of Hydrogen Energy, **2014**, 5, 343-342.

[48] A. Villajos, G. Orcajo, C.Martos, J. Angel, *Co / Ni mixed-metal sited MOF-74 material as hydrogen adsorbent*, International Journal of Hydrogen Energy, **2015**, 40 (15),5346-5352.

[49] SJ. Alesaadi,F. Sabzi, *Hydrogen storage in a series of Zn-based mofs studied by PHSC equation of state.* International Journal of Hydrogen Energy, **2014**, 34, 4234-4241.

[50] S. Niaz,T. Manzoor,A. Hussain, *Hydrogen storage : Materials , methods and perspectives*, Energy Reviews,**2015**,50, 457-469.

[51] Z.Hu,M. Khurana, M. Zhang, D. Zhao, *Ionized Zr-mofs for highly ef fi cient post-combustion CO2 capture.* Chemical Engineering Science, **2015**,4,45-52.

[52] J.Yang,Y. Wang, Z. Zhang, , Journal of Colloid and Interface Science Protection of open-metal V (III) sites, Journal of Colloid And Interface Science, **2015**,29,334-340.

[53] R. Sabouni, H. Kazemian, *Carbon dioxide capturing technologies : A review focusing on metal organic framework materials,*Environmental Science and Pollution Research, **2014**, 21, 5427-5449.

[54] J. Schell, N. Casas, *For pre-combustion CO2 capture by PSA* : adsorption equilibria, **2012**,50,1445-1552.

[55] ED., Dikio,AM., Farah, *Synthesis , Characterization and Comparative Study of Copper and Zinc Metal Organic Frameworks*, Chem Sci Trans., **2013**, 2(4)1386-1394.

[56] YE., Cheon, J. Park, *,Selective gas adsorption in a magnesium-based metal – organic framework*, Chem. Commun., **2009**, 5436-5438.

[57] H. Furukawa, H. Furukawa,KE. Cordova, *The Chemistry and Applications of Metal-Organic Frameworks*, Science, **2013**, 341, 6149-6156.

[58] Y. Li, RT. Yang, *Gas Adsorption and Storage in Metal-Organic Framework MOF-177on and Storage in Metal-Organic Framework MOF-177*. Langmuir, **2007**,18, 342-349.

[59] X. Liu,X.Qu,Q. Shi, *Energetic Characteristics and Magnetic Properties of A*

Three-Dimensional Cobalt (II) Metal-Organic Framework Assembled with Azido and Triazole, Inorg. Chem., **2015**, 54 (23), 11520–11525.

[60] X. Zhao,S. Liu, W. Meng, *Synthesis of magnetic metal- organic framework for efficient removal of organic dyes from water*. Sci Rep. **2015**, 5, 11849.

[61] A.Inayat, A.Badshah, *A copper based metal-organic framework as single source for the synthesis of electrode materials*, International Journal of Hydrogen Energy, **2014**, 39 (34),19609–19620.

[62] F. Jeff, *Using Advances in Electron Microscopy to Study Microbial Interactions*, ,UCLA, **2016**, 124-145.

[63] C. Rivera-Maldonado, *P. Diffraction, Basics of X-ray Diffraction*, X-Ray Powder Diffraction **2007**,1-9.

[64] T. Nicolet, *Introduction to Fourier Transform Infrared Spectrometry*, John Wiley & Sons, **2001**.

[65] M. Ranjbar,*Thermogravimetric Analysis*, Surface & Coatings Technology, **2011**, 205, 4980-4984.

[66] Y. Huang, KS. *Walton, Concepts and Applications: Basic UV-Vis Theory* , Chem. Soc. Rev., **2014**, 43, 6011.

[67] A. Rios,C. Ramos, G. I. Garcia-Acosta, C. M. Lozano-Paulino, *Synthesis, structure, adsorption space and magnetic properties of Ni-oxalate porous molecular magnet"*,. Journal of Materials Science and Engineering, **2012**,14, 557-564.

[68] M.Ali, T.Abbas, *Mg-MOF-74 nanostructures, Journal of Materials Science:* Materials in Electronics, **2015**,2,156-167.

[69] X. Wu,M. Han,G. Xu,B. Liu, *A 3D Ni (II) -MOF with frl topology based on N , N ' -donor co-ligand : Synthesis , structure and magnetic property*, Chem. Soc. Rev., **2011**, 33, 4011-4034.

[70] H. Jasuja,Y. Jiao, *Synthesis of Cobalt , Nickel , Copper , Water Stable Pillared Metal-Organic Frameworks,* Journal of Materials Science and Engineering, **2014**,24, 657-665.

[71] E. Haque, SH. Jhung, *Synthesis of isostructural metal organic frameworks , CPO-27s* , Chemical Engineering Journal, **2011**,18, 2017-2026.

[72]   GW.Peterson, BJ. Schindler, *MOF-74 building unit has a direct impact on toxic gas adsorption,* Chemical Engineering Science,**2011**, 66,2,163–170

[73]   E. Deniz,F. Karadas,HA.Patel, CT. Yavuz, *A combined computational and experimental study of high pressure and supercritical CO2 adsorption on Basolite MOFs*, Microporous and Mesoporous Materials, **2013**, 175, 34-42.

[74]   CC. Wang, JR. Li, *Photocatalytic organic pollutants degradation in metal-organic frameworks*. Energy & Environmental Science, **2014** ,7, 2831-2867

[75]   W. Xu, L. Zhang, S*ynthesis , Structures and Properties of Two Metal-organic Frameworks Derived from 3-Nitro-1 , 2-benzenedicarboxylic Acid,* Korean Chemical Society, **2013**, 34(8), 2375.

[76]   LL. Zhou,X. Feng, L.Ya, *A New Lanthanum Metal-Organic Framework Based on-Phthalate-Acid-Ligand, Synthesis and Reactivity in Inorganic,* Metal-Organic, and Nano-Metal, **2014**,44 (9),1349-1353.

[77]   L. Shi L,L. Hu, *Adsorptive Removal of Methylene Blue from Aqueous Solution using a Ni-Metal Organic Framework,* Journal of Dispersion Science and Technology, **2016**,14, 432-440.

[78]   G. Limousin, *A review on physical bases , modeling and measurement*, Applied Geochemistry, **2007**, 22 (2), 249–275.

[79]   N. Scales,T. Hanley, *A comparative study on adsorption of copper (ii) ions in aqueous solution,* International Journal of Applied Engineering and Technology, **2013**, 3(1), 35-60.

[80]   TL Hanley,Z. Aly, *Removal of aluminium from aqueous solutions using PAN-based adsorbents*,Environmental Science and Pollution Research, **2014**, 21 (5), 3972–3986.

[81]   C. Wu, Synthesis , *characterization , and adsorption kinetics of titania nanotubes for basic dye wastewater treatment*, Adsorption, **2010**, 16 (1), 47–56.